Exposure to negative socio-emotional events induces sustained alteration of resting-state brain networks in older adults

Baez Lugo, Sebastian; Deza, Yacila; Maradan, Christel; Collette, Fabienne; Lutz, Antoine; Marchant, Natalie L.; Chételat, Gaël; Vuilleumier, Patrik; Klimecki-Lenz, Olga Maria; Arenaza-Urquijo, Eider; André, Claire; Botton, Maelle; Cantou, Pauline; Chételat, Gaëlle [**and 23 more**]

How to cite

BAEZ LUGO, Sebastian et al. Exposure to negative socio-emotional events induces sustained alteration of resting-state brain networks in older adults. In: Nature aging, 2023, vol. 3, n° 1, p. 105–120. doi: 10.1038/s43587-022-00341-6

This publication URL: https://archive-ouverte.unige.ch/unige:170199

Publication DOI: 10.1038/s43587-022-00341-6

Title:

Exposure to negative socio-emotional events induces sustained alteration of resting-state brain networks in older adults

Authors:

Sebastian Baez Lugo[1,2,*], Yacila I. Deza-Araujo[1,2], Christel Maradan[2], Fabienne Collette[3], Natalie L. Marchant[4], Gaël Chételat[5], Patrik Vuilleumier[1,2], Olga Klimecki[1,6], and the Medit-Ageing Research Group

Affiliations:

[1] Swiss Center for Affective Sciences, University of Geneva, Geneva, Switzerland.

[2] Laboratory for Behavioral Neurology and Imaging of Cognition, Department of Neuroscience, Medical School, University of Geneva, Geneva, Switzerland.

[3] GIGA-CRC In Vivo Imaging Research Unit, University of Liège, Liège, Belgium.

[4] Division of Psychiatry, University College London, London, UK

[5] Université Normandie, Inserm, Université de Caen-Normandie, Inserm UMR-S U1237, GIP Cyceron, Caen, France

[6] Psychology Department, Technische Universität Dresden, Dresden, Germany.

* Correspondence concerning this article should be addressed to:
sebastian.baezlugo@unige.ch

ABSTRACT:

Basic emotional functions seem well-preserved in older adults. However, their reactivity to and recovery from socially negative events remain poorly characterized. To address this, we designed a novel "task-rest" paradigm in which 182 participants from two independent experiments underwent functional magnetic resonance imaging while exposed to socio-emotional videos. Experiment 1 (N=55) validated the task in young and older participants and unveiled age-dependent effects on brain activity and connectivity that predominated in resting periods after (rather than during) negative social scenes and related to empathy. Crucially, emotional elicitation potentiated subsequent resting-state connectivity between default mode network (DMN) and amygdala exclusively in older adults. Experiment 2 replicated these results in a large older adult cohort (N=127) and additionally showed that emotion-driven changes in posterior DMN-amygdala connectivity were associated with anxiety, rumination, and negative thoughts. These findings uncover the neural dynamics of empathy-related functions in older adults and help better understand how poor social stress recovery may impact neurodegenerative diseases.

Keywords:

Aging, Anxiety, Rumination, Default Mode Network, Functional connectivity, Amygdala, Insula, Posterior cingulate cortex, fMRI.

INTRODUCTION

Aging is a multifaceted process associated with many changes in bodily and mental health. While there is a general decline in physical performances and cognitive abilities in aging [1], emotional functions appear to be maintained or even enhanced in older adults relative to younger adults [2–4]. Indeed, the elderly tend to regulate their emotional states well, a crucial capacity for affective well-being and healthy aging [5]. Unlike younger adults, they often prioritize social and emotional interactions over other goals [6] and show a "positivity bias" in emotion perception [7]. In contrast, maladaptive emotional reactivity and impaired emotion regulation are related to affective psychopathologies such as anxiety, depression, worry, and rumination throughout the lifespan [8,9], including in aging [10]. There is also growing evidence that maladaptive affective styles may represent a significant risk factor for dementia [11–14], one of the primary mental health burdens in the elderly population [15]. However, the neural substrates underpinning proficient socio-affective processing and emotional resilience in the elderly remain unresolved and still scarcely investigated.

An important marker of maladaptive affective style is "emotional inertia", which denotes the degree to which emotions carry over from one moment to the next [16]. Emotional inertia may reflect unsuccessful recovery mechanisms following the offset of affective events and low resilience to stress, associated with higher risks of depression [17,18] and higher trait anxiety and rumination tendencies [19]. Most studies of emotional inertia employed behavioral measures based on experience sampling methods [16,20], e.g., requiring participants to report their affective state at different time points and measuring autocorrelations between successive time-points or events [16,21,22]. More recently, a few neuroimaging studies investigated emotional inertia at the brain level using “task-rest” paradigms [23–29]. In these studies, brain activity is probed not only during active stimulus processing tasks, but also in spontaneous post-task resting periods during which the brain returns to homeostatic balance [30,31]. For example, positive or negative emotions evoked by images or videos were found to induce carryover effects on brain activity and/or connectivity during subsequent resting-state in default mode and affective networks [24,28]. These carryover effects have been observed at different time scales ranging from a few seconds [32] to several minutes [27], following different task instructions ranging from passive viewing through to active regulation of emotions [23], and across different conditions of emotional valence and intensity [25,26].

At the neural level, most brain imaging studies found carryover effects of emotions on the functional dynamics of the default mode network (DMN) either in the form of increased [26,32] or decreased [24,25] activity patterns in regions comprising the medial prefrontal cortex (MPFC), posterior cingulate cortex (PCC), precuneus, and inferior parietal cortex. These regions of the DMN are usually active when individuals are free to let their mind wander in undisturbed conditions [33,34]. Similar effects have also been observed in the insula and amygdala [24]; two regions critically involved in emotional and social processing [35–37]. For instance, a slow recovery of amygdala activity (i.e., longer return to baseline level) after negative images was reported in individuals with higher neuroticism [38]. Slower recovery of amygdala activity after emotional videos was furthermore associated with higher anxiety traits and ruminations [19]. Subcortical limbic regions such as the amygdala and striatum also display sustained changes in their functional connectivity with cortical areas in medial PFC and PCC during rest after negative emotions [24] and reward [28]. These findings converge with studies showing that disturbances in functional connectivity of the amygdala with medial parts of the DMN at rest are associated with anxiety (e.g., decreased connectivity with MPFC [39]) and mood disorders (e.g., increased connectivity with PCC [40]). Taken together, these data suggest that long-lasting carryover effects of emotions on activity and connectivity of limbic networks may provide an important neural marker of emotional regulation style and affective resilience.

However, all previous neuroimaging studies of emotional carryover focused on young healthy participants. It remains unknown whether emotional inertia also occurs in older adults, how it is modified given the well-known "positivity bias" observed in this population [2,3], and how age impacts the functional dynamics of DMN in affective contexts. Indeed, it has been reported that, unlike young adults, older people fail to deactivate the DMN during externally directed cognitive tasks [41] and show increased DMN connectivity with cognitive-related prefrontal regions [42]. Yet, little is known about how aging affects DMN interaction with emotion-related regions, either during or after emotional tasks, and how it relates to other cognitive or socio-affective abilities.

In addition, previous work did not assess whether emotional inertia is modulated by individual differences in empathy, which may strongly influence how people react to negative socio-affective stimuli presented in neuroimaging studies [19,24], and thus how they recover from induced emotions [27]. Because social competencies and affective empathy are relatively

preserved in the elderly [4], socially significant emotional events offer an optimal window to probe emotional reactivity and recovery in this population. Moreover, there is only scarce research on empathy in older people [4,43–47]. Whereas cognitive empathy may decline in older compared to younger people, affective empathy and altruistic behaviors towards others remain intact or even improve [4,47–49]. However, brain responses to seeing others' pain are reduced in anterior insula (AI) and cingulate cortex (ACC) [43], two regions implicated in pain processing, negative affect, and salience detection [36,50]. In contrast, empathy-related responses may increase in superior temporal sulcus (STS) and temporo-parietal junction (TPJ) [46], brain regions frequently associated with Theory of Mind and perspective taking [51]. Yet, despite the importance of social interactions and emotional resilience for healthy aging [52–54], neural substrates underlying the recovery from negative events, as well as their link with empathic skills, personality and psycho-affective traits, have not been investigated during aging.

To address these issues, we designed a novel "task-rest" paradigm combining two lines of research: short (10-18s) empathy inducing videos from the Socio-affective Video Task (SoVT) [55] were shown interspersed with rest periods of 90 seconds (similar to Eryilmaz and colleagues [24]) while participants underwent functional magnetic resonance imaging (fMRI) of brain activity. The SoVT videos consisted of short silent scenes depicting suffering people (high emotion videos) or people in everyday life situations (low emotion videos). By adding short resting-state periods after blocks of videos of each kind, the SoVT-Rest allowed us to evaluate how the aging brain reacts both during and after exposure to emotionally challenging social information. Indeed, defining valid markers of adaptive emotion recovery abilities in a naturalistic paradigm, without making high cognitive demands required by more voluntary/explicit regulation strategies [56], would be valuable to better understand affective resilience mechanisms and better predict affective risk factors associated with pathological aging and dementia [14].

Here, we use the new SoVT-Rest paradigm across two independent experiments to probe for emotion-related carryover effects in large samples of healthy older and young participants. First, we test for differences in the neural substrates of emotional recovery between old and young (Experiment 1), allowing us to validate our paradigm, verify relevant neural effects and assess the effect of age. Next (Experiment 2), we replicate this experiment in a large sample of elderly participants (n=127) in whom we specifically asked whether emotional inertia in brain networks is modulated by empathy and individual traits relevant for

healthy aging, including rumination and anxiety. We hypothesized that exposure to others' suffering (relative to neutral social situations) should (1) engage brain regions implicated in emotional saliency and empathy (i.e., insula, aMCC), but with lower responses in older than young adults [43]; (2) induce subsequent carryover in functional connectivity at rest between emotion-related regions and the DMN, with differential age-dependent patterns; and (3) unveil neural substrates of emotional inertia that may reflect individual variability in anxiety, ruminative thinking, and negative emotions, and thus point to functional biomarkers of affective risk factors for pathological aging [11–14]. In addition, (4) we should observe a "positivity effect" as often reported in older adults [7] and elucidate its relationship to empathy processes during aging.

MATERIAL AND METHODS

Participants

For Experiment 1, a total of 58 healthy participants including 30 younger adults (aged between 19 and 30 years), and 28 older adults (aged between 65 and 78 years) with corrected-to-normal vision, no history of neurological, psychiatric disorder, or alexithymia took part. Thirty participants were expected to participate in each group; however, new research guidelines during the COVID-19 pandemic prevented us from continuing with scanning. Recruitment was performed through social media and advertisement in various locations within the University of Geneva. Three participants were excluded due to a priori exclusion criteria including artifacts in brain images and/or extreme head motion during scanning. The final sample for Experiment 1 included 29 young participants (*M* age= 24, 14 females) and 26 older participants (*M* age = 68.7, 13 females), resulting in a total of N=55 participants (See Table 1 for detailed participants' characteristics). All participants provided written informed consent. This study was approved by the local Swiss ethics committee (commission cantonale d'éthique de la recherche CCRE, Geneva) under the project number 2018-01980.

For Experiment 2, a total of 135 healthy older adults participated, with corrected-to-normal vision and no history of neurological or psychiatric disorders, aged between 65 and 83 years. This session was part of the baseline visit of the Age-Well randomized clinical trial within the Medit-Ageing Project [57], conducted in Caen (France). Detailed inclusion criteria of the Age-Well randomized clinical trial are provided in Supplementary Table 1. Participants were

recruited via advertising in media outlets, social media, and flyers distributed in relevant local events and locations. A total of 8 participants were excluded from the final data analysis due to a priori exclusion criteria: abnormal brain morphology (n = 3), extreme head motion (n = 3), and presence of artifacts in brain images (n = 2). The final sample for this study included 127 participants (M age = 68.8 years, SD = 3.63, 79 females. See Table 1 for other characteristics). All participants provided written informed consent prior to participation. The Age-Well randomized clinical trial was approved by the ethics committee (Comité de Protection des Personnes Nord-Ouest III, Caen, France; trial registration number: EudraCT: 2016-002441-36; IDRCB: 2016-A01767-44; ClinicalTrials.gov Identifier: NCT02977819).

Questionnaires

In order to account for inter-individual differences in psycho-emotional profile, all participants from both experiments answered several questionnaires assessing psycho-affective traits and cognitive functions, including empathy (Interpersonal Reactivity Index, IRI [58]), depression (Geriatric Depression Score, GDS [59] for older adults and Beck Depression Inventory, BDI[60] for younger adults), anxiety (STAI-trait Anxiety Index, STAI [61]), emotion regulation capacities (Emotion Regulation Questionnaire, ERQ [62]), and rumination levels (Rumination Response Scale, RRS [63]). A summary of these questionnaires is provided in Table 1 and Fig. 3. All scores were in the normative range. For a full list of tasks and measures in the Age-Well trial (Experiment 2), please refer to Poisnel and colleagues [57].

TABLE 1. Participant characteristics		Experiment 1			Experiment 2
		Mean (SD) N=55		*P* value for between-group differences [a]	Mean (SD)
		YA Group (n = 29)	OA Group (n = 26)		OA Group N=127
Demographics					
Sex		14 Females	13 Females		79 Females
Age		24.5 (2.67)	68.7 (3.89)		68.8(3.65)
Education (n. of years)		18.4 (1.72)	16.1 (3.4)	0.002	13.21 (3.1)
Psycho-affective traits and Cognitive functions					
STAI	Trait	39.8 (8.31)	36(7.31)	0.08	34.57 (7.12)
Rumination Response Scale [b]	Total	43.5 (10)	36.5 (9.01)	0.008	35.67 (8.55)
	Reflection	11.3 (3.67)	8.77 (3.52)	0.01	8.93 (3.23)
	Brooding	8.97 (2.64)	8.69 (2.41)	0.69	8.06 (2.28)
Interpersonal Reactivity Index	Distress	12 (4.3)	9.62 (5.12)	0.07	10.18 (5.27)
	Empathic Concern	22.1 (3.14)	20.8 (4.24)	0.19	19.76 (4.18)
	Perspective Taking	21.3 (3.71)	17.3 (3.42)	<0.001	17.50 (3.56)
	Fantasy	19.1(4.05)	15.8 (4.08)	0.004	14.35 (4.75)
Emotion regulation abilities	Reappraisal	30.5 (7.11)	29.2 (3.95)	0.4	29.61 (5.79)
	Suppression	12.6 (5.48)	14.8 (4.34)	0.09	16.54 (5.19)
Beck Depression Inventory	Global	5.34 (3.73)			
Geriatric Depression Scale	Global		1.92 (2.3)		1.32 (1.78)

Abbreviations: YA, younger adults; OA, older adults; N, number of total participants in each experiment; n, number of participants in each subgroup; SD, Standard deviation. [a]Between-group differences were assessed using *t*-tests, statistical significance was set to $P < .05$. [b] Values computed on n=126 participants (data missing for one participant).

Socio-affective Video Task-Rest (SoVT-Rest)

The emotion-elicitation task used in both experiments was adapted from the previously validated Socio-affective Video Task (SoVT) [55,64]. The SoVT aims to assess social emotions (e.g., empathy) in response to short silent videos (10-18s). During this task, participants watch 12 High Emotion (HE) and 12 Low Emotion (LE) video clips grouped in blocks of three (see instructions in supplementary Table 2). HE videos depict people suffering (e.g., due to injuries or natural disasters), while LE videos depict people during everyday activities (e.g., walking or talking). In this study, each block was followed by a resting state period of 90 seconds (see instructions in Fig. 1 and supplementary Table 2) in order to assess the carryover effects of emotion elicitation on subsequent resting-state brain activity (similar to Eryilmaz and colleagues [24]). This combination of both paradigms (task and rest) was specifically designed to test for emotional inertia and its relation to empathy. The combined task (SoVT-Rest) is illustrated in Fig. 1.

Overall, three sets (V1, V2, and V3) of 24 videos each were created and randomized across participants. In Experiment 1, the video sets V1, V2, and V3 were seen by n = 21, 18, and 16 participants, respectively. In Experiment 2, these were seen by n = 42, 40, and 45 participants, respectively. During the SoVT-Rest, these videos were presented in two separate runs, with each run followed by a thought probe to assess current mental content during the last rest period (after LE videos in one run and after HE videos in the other run). The order in which runs were presented was randomized so that half of the participants started the experiment with a HE block and the other half with an LE block. The total duration of the SoVT-Rest fMRI paradigm was approximately 21 minutes, consisting of 9.5 min for each run plus 1 minute on average for each thought probe.

After the fMRI session, participants watched all video clips again on a computer outside the scanner and provided ratings on their subjective experience of empathy ("To what degree did you feel the emotions of the characters?") as well as their subjective positive affect ("Indicate the intensity of your positive emotions") and negative affect state ("Indicate the intensity of your negative emotions") (translated from French), for each of the 24 videos. Each scale offered 21 possible responses ranging from 0 ("Not at all") to 10 ("Extremely") with increments of 0.5. The order of questions was always the same: empathy, positive affect, and negative affect. We chose to obtain ratings after fMRI not only to minimize the time older adults spent in the scanner, but also to avoid potential cognitive effects during scanning that may confound neural activity during emotional perception and spontaneous rest recovery periods[65,66].The total time for post-scanning ratings was, on average, 10 minutes. Onset times and response times for both neuroimaging and behavioral tasks were collected via the Cogent toolbox (developed by Cogent 2000 and Cogent Graphics) implemented in Matlab 2012 (Mathworks Inc., Natick, MA, USA).

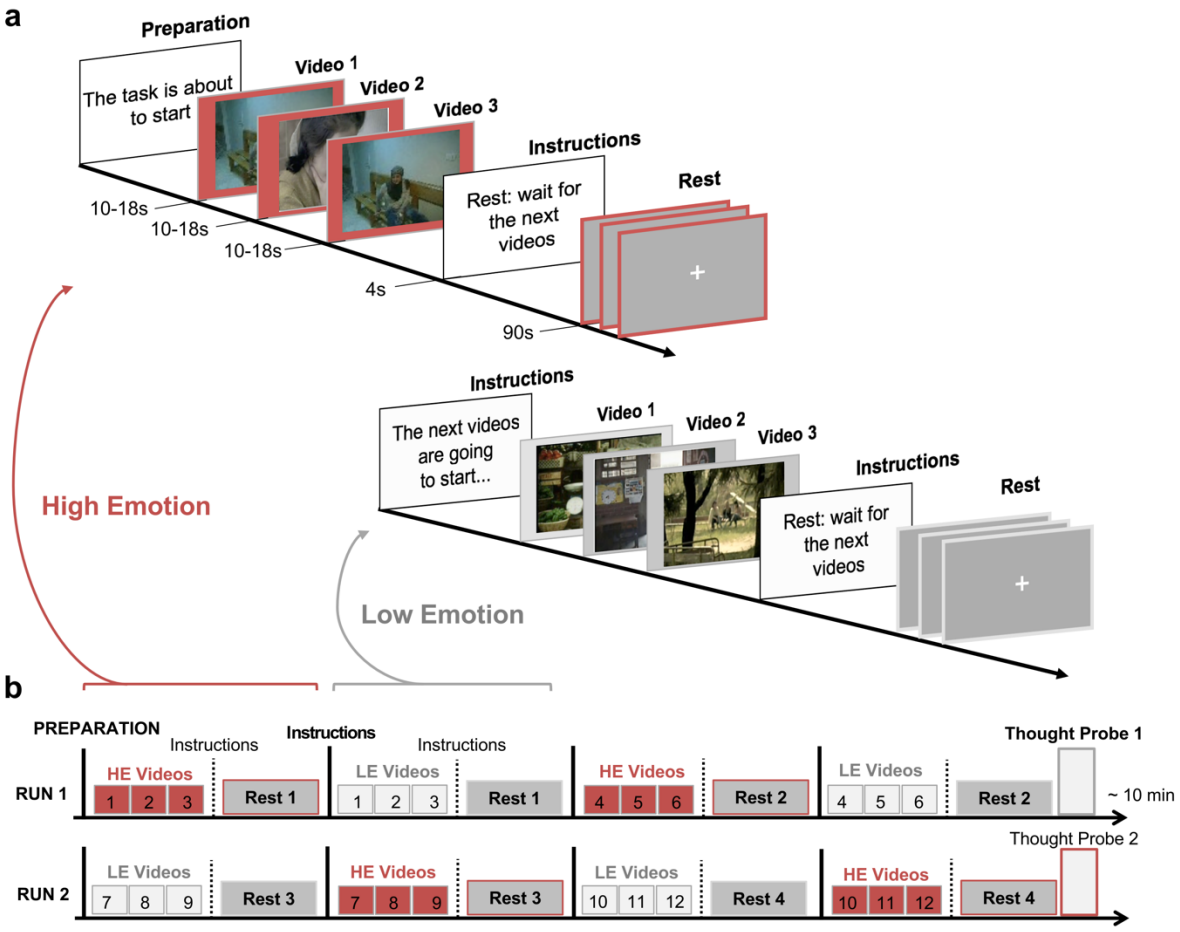

Figure 1. Experimental design: (**a**) SoVT-Rest paradigm: 12 **High Emotion (HE)** and 12 **Low Emotion (LE)** videos were presented grouped in blocks of three. HE videos depict suffering people (e.g., due to injuries or natural disasters), while LE videos depict people during everyday activities (e.g., walking or talking). Each block of three videos is followed by a resting state period of 90 seconds. (**b**) Each run ends with a thought probe in which participants verbally express what they had been thinking and/or feeling during the last rest period (via a microphone), once following a LE block and once following a HE block. The order of the runs was randomized between participants.

Behavioral data analysis.

We performed a repeated measure multivariate analysis of variance (MANOVA, with Pillai's trace statistics) with the within-subject factor "video type" (HE and LE), the between-subject factor "video set" (V1, V2, V3), and three dependent variables: ratings of empathy, positive affect, and negative affect. This was followed up by pairwise *t*-tests. We also computed Spearman's rank correlations between these different scores. Additionally, we performed correlation analyses between ratings of empathy, positive affect, and negative affect of videos and age (as a continuous variable), using non-parametric Spearman's rank correlations because some of these variables were not normally distributed. All statistical analyses are reported with a significance level of $P < 0.05$, and when necessary, P values are corrected for

multiple comparisons using the False Discovery Rate (FDR) method [67]. The statistical analyses were performed with R studio (version 3.6.1) and the corresponding graphs were created with ggplot2 (version 3.2.1).

Acquisition and preprocessing of MRI data.

Experiment 1

Magnetic Resonance Imaging (MRI) scans were acquired at the Brain and Behavior Laboratory of the University of Geneva, using a 3T whole-body MRI scanner (Trio TIM, Siemens, Germany) with the 32-channel head coil. A high-resolution T1-weighted anatomical volume was first acquired using a magnetization-prepared rapid acquisition gradient echo (MPRAGE) sequence (repetition time = 1900 ms; echo time = 2.27 ms; flip angle = 9°; slice thickness = 1 mm; field of view = 256x256 mm^2; in plane resolution = 1x1 mm^2). Blood oxygen level-dependent (BOLD) images were acquired with a susceptibility weighted EPI sequence (TR/TE =2000/30 ms, flip angle = 85°, voxel size (3 x 3 mm), 35 slices, 3 mm slice thickness, 20% slice gap, direction of acquisition = descending). Quality control and preprocessing were conducted using Statistical Parametric Mapping software (SPM12; Wellcome Trust Centre for Neuroimaging, London, United Kingdom) on Matlab 2017 (Mathworks Inc., Natick, MA, USA). Prior to preprocessing, we manually centered all images to the AC-PC axis, aligned the functional and anatomical MRI images, and then realigned all images to the SPM anatomical template. Preprocessing included the following steps: 1) EPI data were realigned to the first volume and spatially smoothed with an 8-mm FWHM Gaussian kernel. 2) Preprocessed fMRI data were denoised for secondary head motion and CSF-related artifacts using automatic noise selection as implemented in ICA-AROMA, a method for distinguishing noise-related components based on ICA decomposition [68]. Additionally, components with high spatial overlap with white matter regions were also removed by means of a linear regression using the fsl_regfilt function of FSL (FMRIB's Software Library, www.fmrib.ox.ac.uk/fsl). 3) Denoised EPI data were coregistered to the anatomical T1 volume. 4) The anatomical T1 volume was segmented and the extracted parameters were used to 5) normalize all EPIs volumes into the Montreal Neurological Institute (MNI) space. This procedure was performed using FSL and SPM12.

Experiment 2

Magnetic Resonance Imaging (MRI) scans were acquired at the GIP Cyceron (Caen, France) using a Philips Achieva (Eindhoven, The Netherlands) 3T scanner with a 32-channel head coil. Participants were provided with earplugs to protect hearing, and their heads were stabilized with foam pads to minimize head motion. A high-resolution T1-weighted anatomical volume was first acquired using a 3D fast field echo sequence (3D-T1-FFE sagittal; repetition time = 7.1 ms; echo time = 3.3 ms; flip angle = 6°; 180 slices with no gap; slice thickness = 1 mm; field of view = 256x256 mm^2; in plane resolution = 1x1 mm^2). Blood oxygen level-dependent (BOLD) images were acquired during the SoVT-Rest task with a T2*-weighted asymmetric spin-echo echo-planar sequence (each run ~10.5 min; TR = 2000 ms, TE = 30 ms, flip angle = 85°, FOV = 240 x 240 mm^2, matrix size = 80 x 68 x 33, voxel size = 3 × 3× 3 mm^3, slice gap = 0.6 mm) in the axial plane parallel to the anterior-posterior commissure. During each functional run, about 310 contiguous axial images were acquired and the first two images were discarded because of saturation effects. Additionally, in order to improve the preprocessing and enhance the quality of the BOLD images [69], T2 and T2* structural volumes were collected. Each functional and anatomical image was visually inspected to discard susceptibility artifacts and anatomical abnormalities.

Quality control and preprocessing were conducted using Statistical Parametric Mapping software (SPM12; Wellcome Trust Centre for Neuroimaging, London, United Kingdom) on Matlab 2017 (Mathworks Inc., Natick, MA, USA). Prior to the preprocessing, we manually centered the images to the AC-PC axis, realigned the functional and anatomical MRI images and then realigned all images to the last version of the SPM anatomical template. The preprocessing procedure was done with SPM12 and followed a methodology designed to reduce geometric distortion effects induced by the magnetic field, described by Villain and colleagues [69]. This procedure included the following steps: 1) realignment of the EPI volumes to the first volume and creation of the mean EPI volume, 2) coregistration of the mean EPI volume and anatomical T1, T2, and T2* volumes, 3) warping of the mean EPI volume to match the anatomical T2* volume, and application of the deformation parameters to all the EPI volumes, 4) segmentation of the anatomical T1 volume, 5) normalization of all the EPIs, T1 and T2* volumes into the Montreal Neurological Institute (MNI) space using the parameters obtained during the T1 segmentation, 6) 8 mm FWHM smoothing of the EPI volumes.

For each individual, frame-wise displacement (FD) [70] was calculated. FD values greater than 0.5 mm were flagged to be temporally censored or "scrubbed" during the first-level analysis (see description below). The average of FD volumes censored was M = 6.8 (SD = 8.3, Min = 1 , Max = 38) for both runs for a total of n=65 participants. Three participants were excluded from further analysis because >10% of volumes a FD > 0.5 mm within one run.

General linear model analysis with SPM

For both experiments, the MRI SoVT-Rest data was analyzed using General Linear Models in SPM12 (implemented in Matlab 2017). This comprised standard first-level analyses at the subject level, followed by random effect (2nd-level) analyses to assess the effects of interest at the group level. For the 1st-level analysis, a design matrix consisting of two separate sessions was constructed for each participant. Experimental event regressors in each session included the fixation cross (10 sec), instructions (8 sec in Experiment 1, 4 sec in Experiment 2), the three videos (~15 sec each) modeled separately, and the rest periods following each block (90 sec). Each rest period was divided into three equal parts (30 sec time bins) in order to model different time intervals during which brain activity may gradually change after the end of the HE and LE video blocks (similar to Eryilmaz and colleagues [24]).

The different regressors were then convolved with a hemodynamic response function (HRF) according to a block design for univariate regression analysis. The six realignment parameters were added to the matrices in order to account for motion confounds, and low-frequency drifts were removed via a high-pass filter (cutoff frequency at 1/ 256 Hz). The final 1st-level matrix consisted of 2 sessions of 21 regressors each (1 fixation cross + 1 instruction for videos + 1 instructions for rest + 3 HE videos + 3 post HE rest + 3 LE videos + 3 post LE rest + 6 motion parameters). Additionally, we addressed the influence of remaining motion on BOLD data by performing data censoring as described by Power and colleagues [70]. Specifically, during the estimation of beta coefficients for each regressor of interest, volumes with FD >0.5 mm were flagged in the design matrices and ignored during the estimation of the 1st -levels.

For the 2nd-level analyses, we used flexible factorial designs where the estimated parameters from 1st-level contrasts of interest were entered separately for each subject. The second-level design matrix was generated with SPM12 and included 12 regressors of interest (3 HE videos + 3 Post HE rest + 3 LE videos + 3 Post LE rest). This step allowed us to

investigate the effect of each experimental condition on brain activity, including the main condition effects (video and rest), the specific emotional effects (HE and LE) during either the video or the subsequent rest periods as well as the age effect on the different conditions (young vs. old, Experiment 1).

In both experiments, we conducted *t*-tests contrasts to compare the conditions of interest (videos vs. rest periods and vice versa) and the specific emotional effects (videos: HE vs. LE; rest: HE vs. LE). In Experiment 1, we additionally tested for age differences in these effects (OA vs. YA (videos: HE vs. LE); OA vs. YA (rest: HE vs. LE)). In Experiment 1, results are reported at P uncorrected < 0.001, k > 20 which has been shown to be acceptable and reliable for fMRI experiments assessing cognitive and affective processes with unprecise onsets [71], and clusters surviving whole-brain family-wise error correction at $P < 0.05$ at the cluster level (FWEc) are indicated in figures and tables (see supplementary Table 3a). In Experiment 2, all comparisons are reported with a whole-brain FWE correction at $P < 0.05$, at the voxel level (see supplementary Table 3b).

Functional connectivity analysis during rest periods, definition of Regions of Interest (ROI), and the data analysis pipeline

For both experiments, we conducted functional connectivity analyses between the most important brain regions of interest (ROIs) associated with the empathy network and with the default mode network (DMN). In addition, we also included the bilateral amygdalae among regions used for this analysis because previous studies assessing carryover effects in the brain have related sustained amygdala activity to anxiety traits [19] and emotional reactivity [38]. For nodes of the DMN, we chose the posterior cingulate cortex (PCC) and the anterior medial prefrontal cortex (aMPFC), following Andrews-Hanna and colleagues [72]. Based on the results of a meta-analysis by Fan and colleagues [50], the bilateral anterior insula (AI) and anterior medial cingulate cortex (aMCC) were used as ROIs in the empathy network. Time series were extracted from 6 mm-radius spheres around the peak of each of these ROIs. The amygdala was defined anatomically using the current SPM anatomical template provided by Neuromorphometrics, Inc (http://Neuromorphometrics.com/).

Functional connectivity analyses were performed using Matlab 2017 and R studio (version 3.6.1). For each participant, time courses of activity (from each voxel of the brain) were high-pass filtered at 256 Hz, detrended and standardized (Z-score) before extracting specific time courses from the defined ROIs. In addition, white matter (WM), cerebrospinal

fluid (CSF) signals, and realignment parameters were included as nuisance regressors in Experiment 2. For each participant, time series from the instructions and videos periods were removed, and the remaining time series corresponding to the rest periods were concatenated. This procedure was previously proposed by Fair and colleagues [73] and proved to be qualitatively and quantitatively very similar to continuous resting-state data. Additionally, to correct extreme head motion without affecting the autocorrelation of the time series, image volumes flagged with FD > 0.5mm were removed and replaced by interpolation (every flagged volume X was replaced by the estimated mean of the X-1 and X+1 volumes). The final concatenated time series resulted in 184 frames (~386 s) of resting-state data for each subject.

We then correlated the time-courses between the different ROIs using Pearson correlations [74], and the resulting coefficients were Fisher's *r* to *z* transformed in order to improve normality in the data. Individual *Z*-score maps (correlation matrices) were created for each participant (see Fig. 2a,b,c). To test for significant differences between the two correlation matrices (post HE rest and post LE rest), we used a non-parametric permutation test [75]. For each pair of nodes, the permutation test compared the true correlation difference (e.g., HE - LE) to a null distribution built by randomly flipping the sign of the correlation coefficients and computing the difference many times (n=5000) (see Fig. 2d). More precisely, for each pair of nodes (e.g., HE - LE for ROI 1 and ROI 3), a vector of values of n=number of participants was obtained and a one-sample *t*-test was computed to obtain the real *t* value (t_{real}). Then, the signs of the elements in the vector were randomly flipped (n=5000) and the model was fitted repeatedly once for every flipping. For each fit, a new realization of the *t* statistic was computed so that an empirical distribution of *t* under the null hypothesis was constructed ($t_{permuted}$). From this null distribution, a *P* value was computed by assessing the probability of the t_{real} to be higher than 95% of the values on the empirical $t_{permuted}$ distribution [75]. Finally, the obtained *P* values were converted into an equivalent *Z*-score and significant changes (marked by asterisk in matrices) were retained for $Z > 1.64$ (equivalent to $P < 0.05$, one-tailed given observed increases without decreases in GLM analysis, uncorrected).

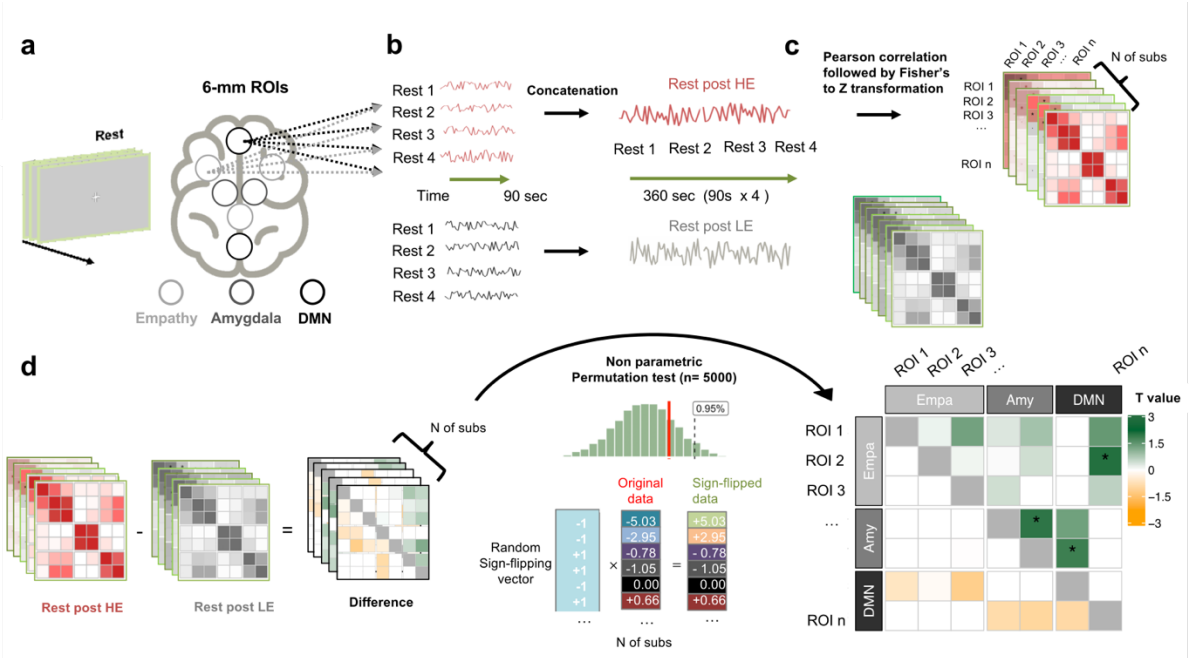

Figure 2. Functional connectivity pipeline: (**a**) Regions of interest (ROIs) from the default mode network (DMN) were chosen based on Andrews-Hanna et al. (2010), including the posterior cingulate cortex (PCC, -8 -56 26) and anterior medial prefrontal cortex (aMPFC, -6 52 -2). ROIs from the empathy network (Empa) were based on the meta-analysis by Fan et al. (2011), including the bilateral anterior insula (AI, -36 16 2 and 38 24 -2) and anterior mid cingulate cortex (aMCC, -2 24 38). A 6 mm-radius sphere was created for each ROI**.** The amygdalae (Amy) were defined anatomically using the SPM anatomical template. (**b**) For every participant, time-series from the video and instruction periods were removed, and the remaining time series corresponding to the rest periods were concatenated [73]. The final concatenated time series of the four rest blocks for each type of video (high emotion, HE or low emotion, LE) resulted in 184 frames (~360 s) of resting-state data for each subject. (**c**) We then correlated the time-courses between the different ROIs using Pearson's *r* correlation, and the resulting coefficients were Fisher's *r* to *z* transformed to improve normality in the data. Individual *Z*-score maps (correlation matrices) were created for each participant. (**d**) Finally, significant differences between the two correlation matrices (Rest post HE vs. Rest post LE) were tested using a non-parametric permutation test [75]. For each pair of nodes, the permutation test compared the true correlation difference t_{real} (HE vs. LE) to a null distribution $t_{permuted}$ constructed by randomly flipping the sign of the correlation coefficients and repeating the *t* statistic (n=5000).

Thought probes

For each participant in Experiment 2, two thought probes were recorded after the last rest period of each run and subsequently analyzed to test for differences in spontaneous mind wandering after emotional videos. Participants freely described their thoughts, and these narratives were digitally recorded and transcribed for analyses by two independent raters (see suppementary Table 4). For each probe (post HE rest and post LE rest), the two raters attributed the presence (Present) or the absence (Absent) of specific thought contents according to a diverse set of pre-defined categories (Supplementary Table 4). These categories were selected according to a priori relevant affective or cognitive dimensions, and included the following: *negative* and *positive emotion*s, *directed attention to oneself* and *to others*, *emotion regulation (voluntary control of emotions)*, *negative* and *positive social emotions, rumination,* and *temporality (present or past/future)*. Categories with low variability (i.e., the same thought content reported by more than 85% of participants) were not included in further analyses since this prevented reliable regression analysis (for details, see supplementary Table 4). The final dimensions included *negative* and *positive emotion*s, *directed attention to oneself* and *to others,* and *positive social emotions*. This final analysis of thought probes comprised data from 109 participants for rest periods after HE videos and 110 participants for the rest periods after LE videos. This was due to i) missing thought probes for 9 participants and ii) exclusion of reports that did not refer directly to thoughts or feelings in the rest period (but rather to factual details in the videos) for both runs (n = 5), following LE rest (n = 3) or following HE rest (n = 4). Interrater agreement on the final dimensions ranged from 0.28 to 0.66 (Cohen's kappa index; supplementary Table 4 for details). The statistical analyses were performed with R studio (version 3.6.1) and the corresponding graphs were created with ggplot2 (version 3.2.1).

RESULTS

Participants characteristics

Participants' characteristics, including demographical data, psycho-affective traits, cognitive abilities, socio-emotional questionnaires, as well as corresponding age differences, are provided in Table 1 and Fig. 3. Older vs. younger participants (Experiment 1) did not differ in trait anxiety, affective empathy, and emotion regulation scores. However, older adults reported lower scores of cognitive empathy as measured by the perspective-taking subscale (t_{53} = 4.2, P < 0.001, d = 1.13, two-tailed) and the fantasy scales of the IRI ($t_{52.3}$ = 3, P = 0.004, d = 0.81, two-tailed). Older adults also had lower scores in reflective rumination ($t_{52.7}$ = 2.62, P = 0.01, d = 0.7, two-tailed). The two independent older adults samples (Experiment 1 and Experiment 2) did not differ in any of the scores (all $t \leq 1.6$, all $P \geq 0.09$).

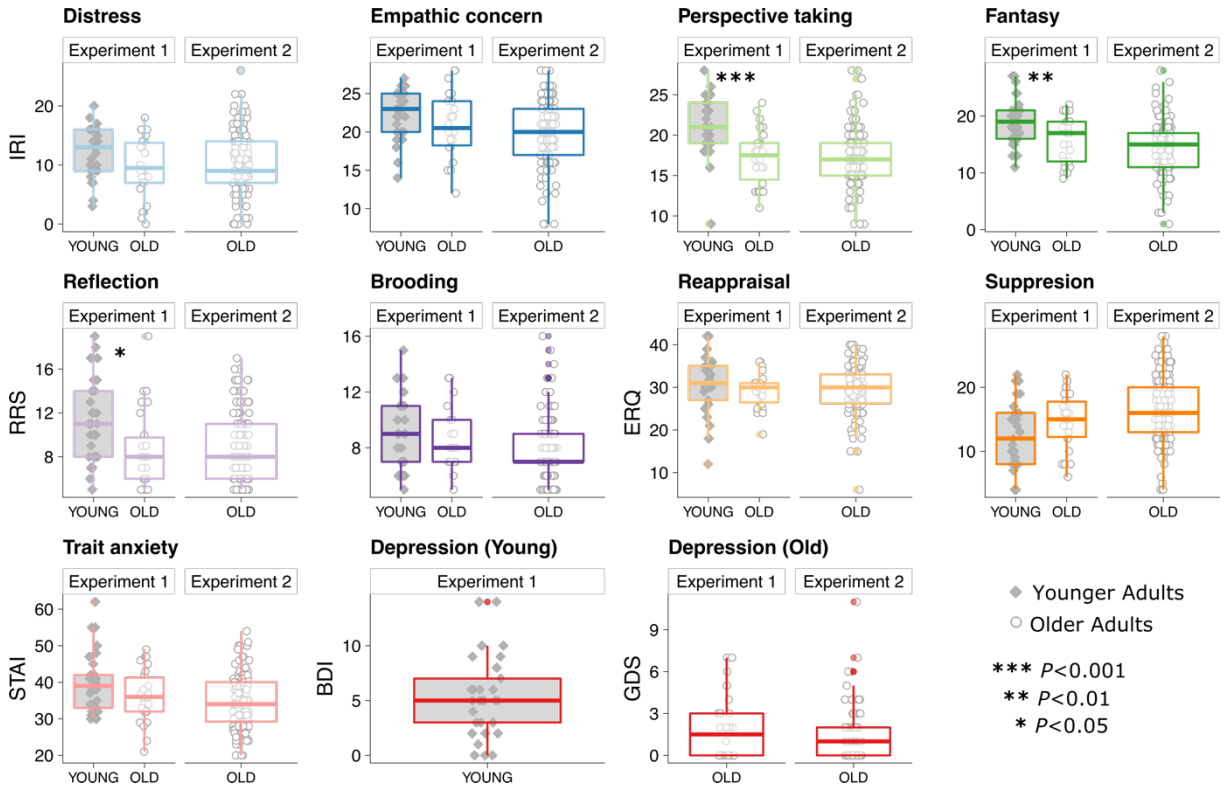

Figure 3. Participants' characteristics in terms of psycho-affective traits and socio-emotional competencies for both Experiment 1 (n=29 younger and n=26 older adults) and Experiment 2 (N=127 older adults). Age-related differences (Experiment 1) were tested with *t*-tests and significant results are marked with *. Grey diamonds= younger adults, white dots= older adults. IRI: Interpersonal Reactivity Index, GDS: Geriatric Depression Score (for older adults only), BDI: Beck's Depression Inventory(for younger adults only), STAI: STAI-trait Anxiety Index, RRS: Rumination Response Scale, ERQ: Emotion Regulation Questionnaire.

Behavioral responses of the SoVT-Rest task

Reliability of the three parallel video sets

To check whether the three video sets elicited similar emotional responses, we performed repeated measures multivariate analysis of variance (MANOVA, with Pillai's trace statistics) with the within-subject factor "video type" (HE vs LE), the between-subject factor "video set" (V1, V2, V3), and three dependent variables: empathy, positive affect, and negative affect ratings. As expected, and replicating results from Klimecki and colleagues [55], these analyses revealed no significant differences between the three video sets for any of the self-reported ratings for Experiment 1 (Pillai's trace = 0.07, $F(6,102) = 0.7$, $P = 0.6$) nor for Experiment 2 (Pillai's trace = 0.07, $F(6,246) = 1.41$, $P = 0.2$) (see supplementary Fig. 1).

Impact of high compared to low emotion videos and aging effects on affective and empathy ratings

In Experiment 1, we compared the effects of HE and LE videos using pairwise *t*-tests for each of the three affective ratings (empathy, positive, and negative affect). These findings were fully replicated in Experiment 2. As predicted, participants reported higher levels of empathy (Exp 1: $t_{54} = 14.35$, $P < 0.001$, $d = 1.67$, two-tailed ; Exp 2: $t_{126} = 14.5$, $P < 0.001$, $d = 1.31$, two-tailed), higher negative affect (Exp 1: $t_{54} = 23.35$, $P < 0.001$, $d = 3.77$, two-tailed; Exp 2: $t_{126} = 26.9$, $P < 0.001$, $d = 2.89$, two-tailed), and lower positive affect (Exp 1: $t_{54} = -16.85$, $P < 0.001$, $d = -2.31$, two-tailed; Exp 2: $t_{126} = -18.9$, $P < 0.001$, $d = -2.31$, two-tailed), when presented with HE as compared to LE videos (see Fig. 4a). Importantly, the reported differences between HE > LE conditions on these ratings were not affected by sex in any of the experiments (see supplementary Fig. 6). These data validate a successful elicitation of socio-emotional responses with the SoVT-Rest.

Additionnaly, Experiment 1 allowed us to determine age-dependent differences in affective and empathy ratings in the SoVT-Rest task. First, independent ANOVAs showed significant main effects of age on empathy ($F(1,53) = 10.8$, $P = 0.002$) and positive affect ($F(1,53) = 24$, $P < 0.001$), but not on negative affect ($F(1,53) = 1.01$, $P = 0.3$). Follow-up two-sample *t*-tests revealed that in contrast to younger adults, older adults reported higher levels of empathy only for LE videos $t_{51.5} = 4.45$, $P < 0.001$, $d = 1.19$, two-tailed) as well as higher positive emotions

for both HE videos ($t_{36.5}$ = 4.63, P < 0.001, d = 1.29, two-tailed) and LE videos ($t_{50.1}$ = 3.68, P < 0.001, d = 0.98, two-tailed). Interestingly, the two independent older samples (Experiment 1 and Experiment 2) did not differ in any of the scores (all $t \leq 1.8$, all other $P \geq 0.07$) (see Fig. 4a) except for even higher ratings of empathy for LE videos in the elderly from Experiment 2 than those from Experiment 1 (t_{36} = 2.20, P = 0.03, d = 0.47, two-tailed).

We further tested whether age effects on affective ratings were observed within each age group independently (young and older participants). Spearman correlations were computed between age (as a continuous variable) and empathy, positive affect, and negative affect for each age group (collapsing both older adults samples from Experiments 1 and 2). This analysis revealed that during HE videos, age correlated negatively with negative affect (*rho* = -0.2, P_{FDR} = 0.03) and positively with positive affect (*rho* = 0.25, P_{FDR} = 0.006) in older individuals, but not in younger adults. In addition, age correlated positively with empathy for LE videos in the young (*rho* = 0.44, P_{FDR} = 0.03), but not older adults (Fig. 4b).

These analyses were repeated excluding n=8 older adults that reported "moderated" levels of depression according to a threshold of GDS >5 [76]. Results did not change (see supplementary Table 5). We, therefore, decided not to exclude them from the main analyses.

Correlation between empathy and affective valence during the SoVT-Rest

To test how empathy was associated with positive and negative affect during HE and LE videos, we computed Spearman correlations between these rating scales. For both younger and older adults, empathy increased with higher negative affect during HE videos (YOUNG : *rho* = 0.86, P_{FDR} < 0.001; OLD: *rho* = 0.63, P_{FDR} < 0.001) and with higher positive affect during LE videos (YOUNG: *rho* = 0.75, P_{FDR} < 0.001; OLD: *rho* = 0.65, P_{FDR} < 0.001). Interestingly, during HE videos, empathy correlated negatively with positive affect for older (*rho* = -0.35, P_{FDR} < 0.001) but not younger adults (*rho* = 0.27, P_{FDR} = 0.18); whereas during LE videos, empathy correlated positively with negative affect for the younger (*rho* = 0.63, P_{FDR} < 0.001) but not the older (*rho* = 0.13, P_{FDR} = 0.14) (Fig. 4c).

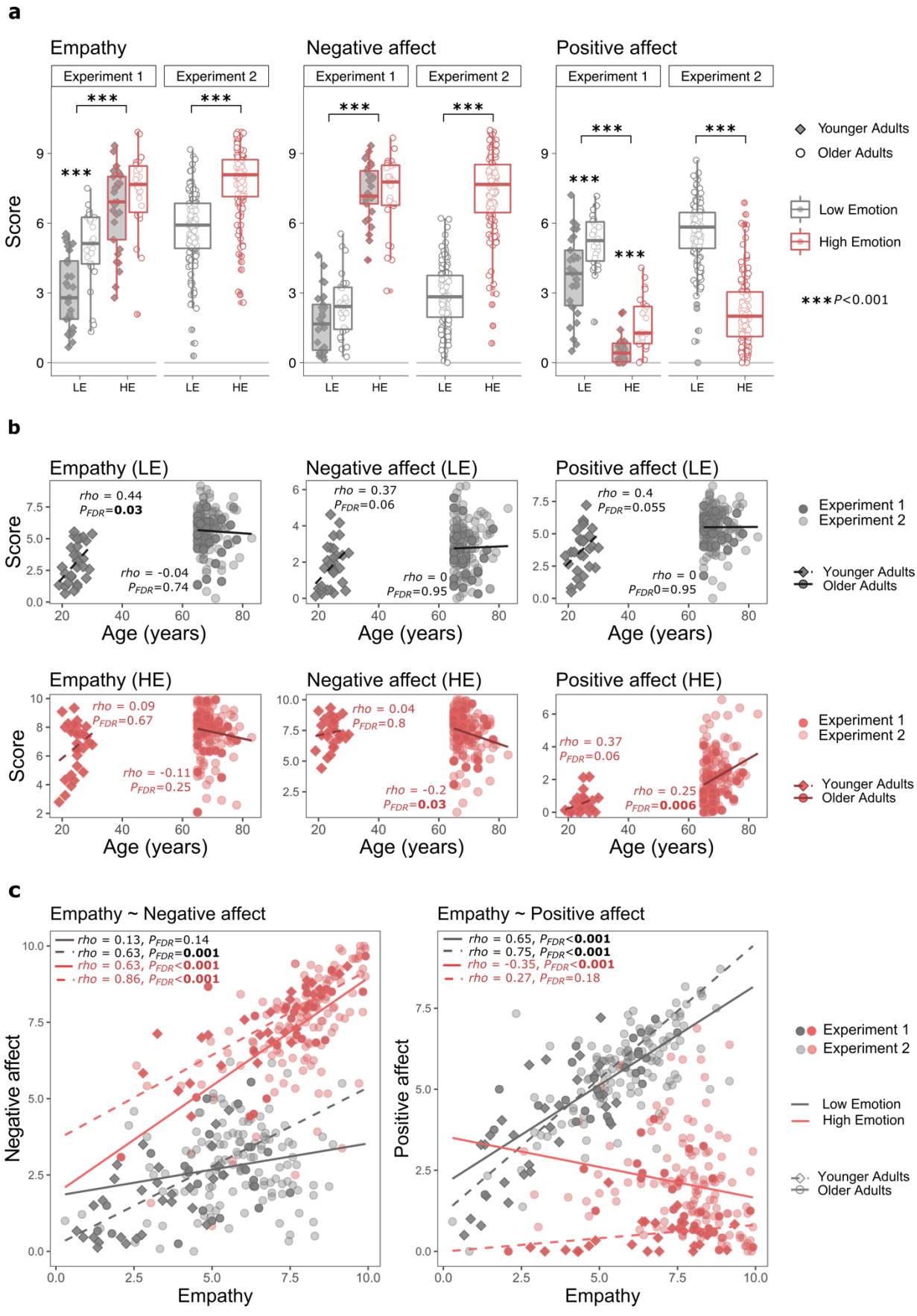
a
Empathy
Negative affect
Positive affect
Experiment 1
Experiment 2
Score
LE
HE
***
Younger Adults
Older Adults
Low Emotion
High Emotion
***P<0.001
b
Empathy (LE)
Negative affect (LE)
Positive affect (LE)
rho = 0.44
P_FDR=0.03
rho = -0.04
P_FDR=0.74
rho = 0.37
P_FDR=0.06
rho = 0
P_FDR=0.95
rho = 0.4
P_FDR=0.055
rho = 0
P_FDR0=0.95
Age (years)
Empathy (HE)
Negative affect (HE)
Positive affect (HE)
rho = 0.09
P_FDR=0.67
rho = -0.11
P_FDR=0.25
rho = 0.04
P_FDR=0.8
rho = -0.2
P_FDR=0.03
rho = 0.37
P_FDR=0.06
rho = 0.25
P_FDR=0.006
c
Empathy ~ Negative affect
Empathy ~ Positive affect
rho = 0.13, P_FDR=0.14
rho = 0.63, P_FDR=0.001
rho = 0.63, P_FDR<0.001
rho = 0.86, P_FDR<0.001
rho = 0.65, P_FDR<0.001
rho = 0.75, P_FDR<0.001
rho = -0.35, P_FDR<0.001
rho = 0.27, P_FDR=0.18
Negative affect
Positive affect
Empathy

563

Figure 4. (**a**) Self-reported scores of empathy, positive affect, and negative affect for the high emotion (HE) and low emotion (LE) videos across experiments. Significant differences between age groups or video type are marked by *** representing $P < 0.001$ (**b**) Scatter plots illustrating Spearman correlations between age and scores of empathy, positive affect, and negative affect. (**c**) Scatter plots illustrating Spearman correlations between scores of empathy and affective ratings. Correlations for (b) and (c) were computed together; therefore, *P* values are reported corrected for multiple comparisons using the false discovery rate (FDR) method. Significant *P* values are marked in bold. Dots represent averaged values for each participant per condition; Dots/solid line: older adults, diamonds/dashed line: younger adults; $n_{Exp1} = 55$, $n_{Exp2} = 127$; Red: HE videos, Grey: LE videos.

Neural responses of the SoVT-Rest task

Main effects of videos and rest periods (manipulation check)

We first verified that video and rest periods induced differential brain activity by testing for the main effects of task conditions. As expected, comparing videos versus rest periods (Videos > Rest, voxel-wise $P < 0.05$ FWE-corrected) revealed greater activity in widespread networks, including stronger increases in visual cortices. Conversely, comparing rest versus video watching periods (Rest > Videos, voxel-wise $P < 0.05$ FWE-corrected) revealed greater activity in several regions typically associated with the default mode network, such as the PCC/Precuneus, ACC/MPFC, and bilateral IPL. These results were similar in Experiments 1 and 2 (see supplementary Fig. 2).

Brain regions activated when faced with others' suffering and age-related differences

In Experiment 1, we determined the effect of the emotional content of videos (high, HE vs. low, LE) in each age group, as well as age-related differences. In both groups, the contrast of HE > LE conditions (voxel-wise $P < 0.05$ FWEc-corrected; and $P < 0.001$ uncorrected, k=20) demonstrated consistent increases in temporo-parietal junction (l.TPJ), right inferior frontal gyrus (r.IFG), as well as temporal and occipital cortices (see Fig. 5a and supplementary Table 3a). Older adults showed larger activations in PCC and dMPFC, whereas younger adults showed additional increases in AI and PAG (see Fig 5a). A direct between-group comparison (2x2 ANOVA) revealed that the older adults more strongly engaged cortical regions in bilateral angular gyrus (TPJ/IPL) and dLPFC. Inversely, the young more strongly engaged subcortical areas in ventral striatum and PAG, as well as sensory areas in parietal and occipito-temporal cortices (Fig 5b).

Experiment 2 replicated the results found in older adults from Experiment 1, surviving a more stringent statistical threshold due to the larger sample size. Indeed, HE > LE videos (voxel-wise $P < 0.05$ FWE-corrected) induced greater activity in fronto-parietal and midline regions including left TPJ, dMPFC, and PCC, together with significant increases in bilateral anterior insula (AI), anterior cingulate cortex (ACC), anterior mid-cingulate cortex (aMCC), and ventral striatum (VS) (see Fig. 5c, and supplementary Table 3b).

Overall, brain activations found across the two experiments overlap with networks classically associated with empathy [36,50], compassion [55,64,77], as well as cognitive and affective theory of mind [51,78].

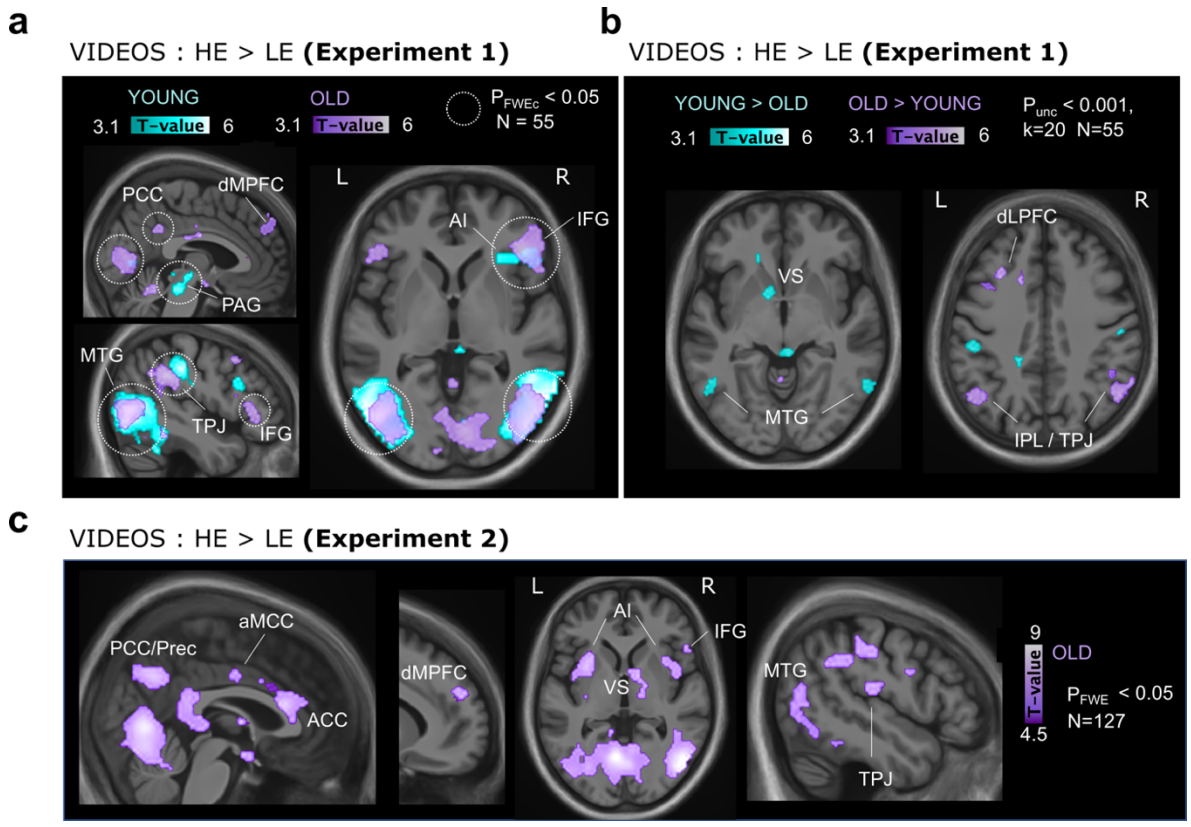

Figure 5. Brain regions with greater activation during high emotion (HE) videos in contrast to low emotion (LE) videos across experiments and age groups. **(a)** Brain maps for younger (n=29) and older (n=26) adults in Experiment 1. **(b)** Between age-groups difference in Experiment 1. For display purposes, results are thresholded at P uncorrected < 0.001, with a minimum cluster size of (k = 20). Clusters surviving correction for multiple comparisons (P FWE < 0.05 at the cluster level) are surrounded in white dotted circles. **(c)** Brain maps for older adults (N=127) in Experiment 2. Results survived familywise error (FWE) correction at the voxel level ($P < 0.05$ FWE-corrected). Overall HE > LE videos activated regions previously reported as part of the empathy network (bilateral anterior insula, AI; anterior middle cingulate cortex, aMCC), and regions comprised in the Theory of Mind network (PCC: posterior cingulate cortex, l. TPJ: left temporo-parietal junction, dMPFC: dorsal medial prefrontal cortex) and the Compassion network (VS: ventral striatum) [77,79].

Older adults show carryover effects of socio-emotional videos during subsequent rest periods

To test for carryover effects of emotional videos on subsequent resting state [24] and thus assess homeostatic emotion regulation abilities [16], we compared rest periods after HE videos to rest periods after LE videos. In Experiment 1, this contrast (post HE > post LE; voxel-wise $P < 0.001$ uncorrected, k=20) revealed greater brain activations mostly in the older group, involving the medial prefrontal cortex (MPFC), left anterior insula (l.AI), right inferior frontal gyrus (r.IFG), several temporo parietal cortices, as well as right hippocampus (r.Hipp) (see Fig. 6a and supplementary Table 3a). The same contrast in younger adults showed more limited increases predominating in MCC (see supplementary Table 3a). A direct between-group comparison (2x2 ANOVA) confirmed that older adults engaged these regions (AI, IFG, dMPFC) more strongly, with further significant effects in left MTG and left amygdala, wheras the younger showed higher activity predominating in left hippocampus and precentral motor regions (see Fig 6b and supplementary Table 3a).

In Experiment 2, similar regions were found, again surviving a more stringent statistical threshold and replicating our results in older adults from Experiment 1. The contrast post HE > post LE (voxel-wise $P < 0.05$ FWE-corrected) highlighted higher resting activity mainly among midline nodes of the DMN (ACC/dMPFC, and Precuneus/PCC), as well as increases in the right amygdala (r.AMYG) and the ventral part of the right anterior insula (r.AI) (see Fig. 6c and supplementary Table 3b).

The larger sample size in Experiment 2 allowed us to conduct additional analyses to assess whether these carryover effects at rest directly resulted from higher activity in the same regions during videos periods. To this aim, we identified voxels that were most reliably activated for a specific contrast (HE > LE) across the two periods (videos and rest) by applying an inclusive mask from one contrast (e.g., videos: HE > LE) to the other contrast (rest: post HE > post LE) with a strict threshold used for both ($P < 0.00001$). This overlap of emotional increases (contrasts HE>LE) from both the videos and the rest periods allowed us to determine common areas of activity, shared across the task conditions (Fig. 6c). This analysis revealed a restricted overlap in a few selective regions, mainly dMPFC and PCC,

where voxels with emotional activation during videos also exhibited emotional carryover effects at rest after videos, suggesting sustained increases persisting over time (Fig. 6e,f). In contrast, other regions differentially activated during emotional videos did not display any carryover effects during the subsequent rest periods (i.e., exclusively responding to HE > LE conditions during the videos periods), including not only visual cortical areas but also mid cingulate areas (MCC; Fig. 6d). Interestingly the right amygdala as well as a segment of the right anterior insula (ventral part) did not show significant differences for the HE > LE contrast during videos but were robustly activated in the post HE > post LE rest periods (Fig. 6g,h). These dissociations between rest and video-related activity are further illustrated by plots of brain activity (contrasts estimates) over time across the different task periods (using a single time bin of ~45 sec during videos and three successive time bins of 30 seconds during rest to depict the time course of the activation) and the different conditions (HE and LE videos) (Fig. 6d,e,f,g,h).

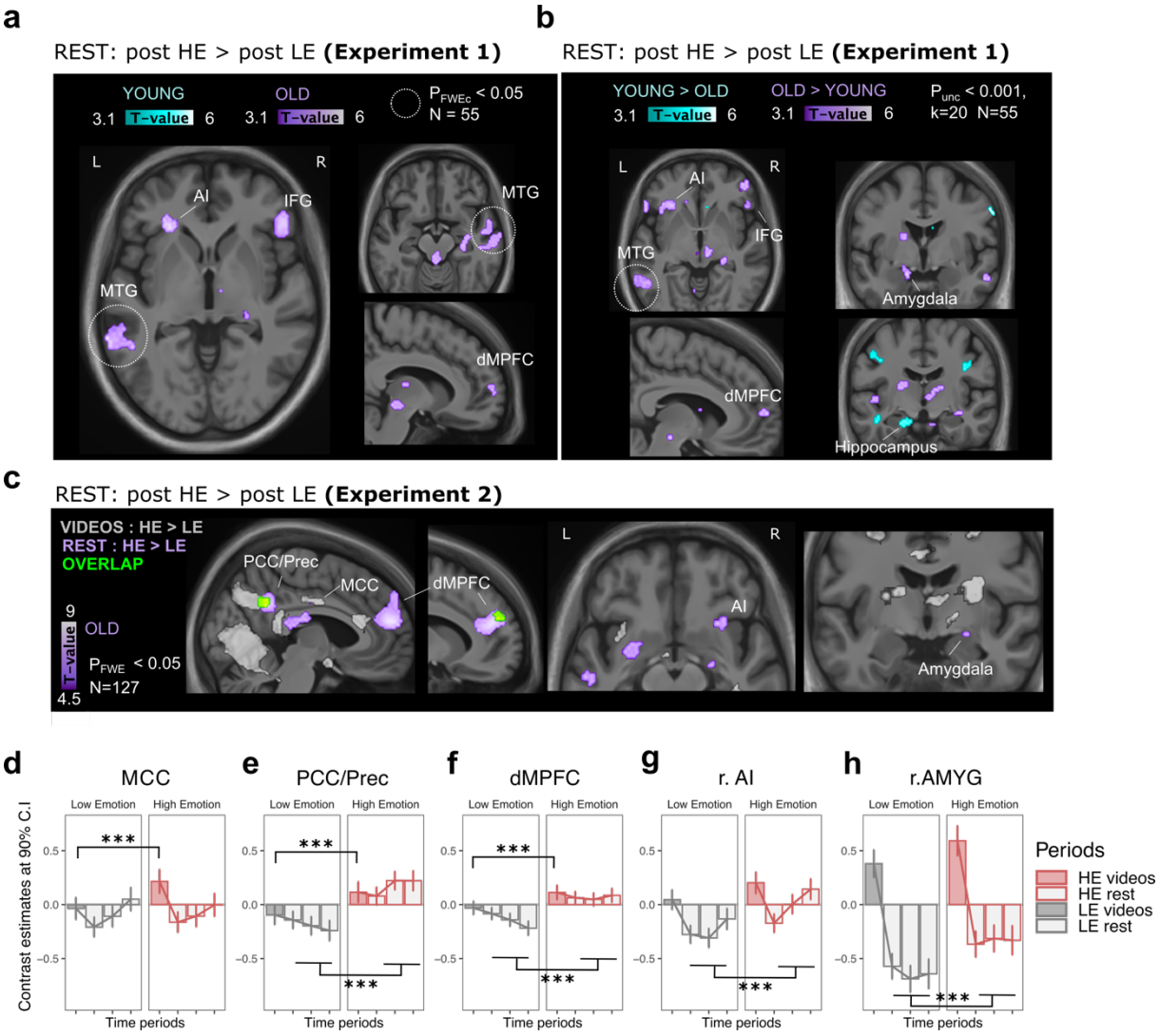

Figure 6. Carryover effects on brain activity at rest subsequent to high emotion (post HE) versus low emotion (post LE) videos across experiments and age groups. (a) Brain maps for younger adults (n=29, blue clusters) and older adults (n=26, violet clusters) in Experiment 1. (**b)** Direct comparisons of brain maps representing significant age-related differences in Experiment 1. Results are thresholded at *P* uncorrected < 0.001, with a minimum cluster size of (k = 20). Clusters surviving correction for multiple comparison (*P* FWE < 0.05 at the cluster level) are surrounded in white dotted circles. (**c**) Brain activations for older adults (N=127) in Experiment 2. Violet cluster show significant increases in rest periods for the contrast post HE > post LE. Green clusters show the overlap of these activations with emotional effects observed during videos (shown in grey). Results are thresholded at $P < 0.05$ corrected for multiple comparisons using family-wise error (FWE) correction at the voxel level. (**d,e,f,g,h**) Magnitude and time-course of brain activity (parameter estimates) for relevant regions during the different task periods in Experiment 2. (**d**) Example of a region (in MCC) responding to HE vs LE videos, but showing no significant difference during rest after HE vs LE videos. (**e,f**) Example of regions (PCC/Prec and dMPFC) responding to HE > LE videos and showing significant carryover with sustained activity during subsequent rest. (**g,h**) The right amygdala as well as the ventral part of the right anterior insula did not reliably respond to HE vs LE videos but showed significant increases in activations during corresponding rest. Grey lines track activity time-courses during LE conditions. Pink lines track activity time-courses during HE conditions. Grey and pink bars indicate activity (blocks of 3 videos = ~45 seconds) for LE and HE videos respectively, white bars indicate activity (over 3 bins of 30 seconds) during rest periods subsequent to corresponding videos periods. *** $P < 0.05$ FWE-corrected. PCC: posterior cingulate cortex, Prec: precuneus, MCC: mid-cingulate cortex, ACC: anterior cingulate cortex, dMPFC: dorsomedial prefrontal cortex, r. ventral AI: right anterior insula (ventral part), r. AMYG: right amygdala, IFG: inferior-frontsal gyrus, MTG : middle temporal gyrus, Hipp: Hippocampus.

Exposure to others suffering impacts subsequent brain network connectivity in older but not younger adults

To further assess the lingering impact of emotional videos on brain activity dynamics (emotional inertia), we examined differences in functional connectivity between and within a priori defined networks. To do so, we first determined the functional connectivity patterns in regional time-series from the default mode network, the empathy network, and bilateral amygdala measured during the rest periods after HE videos, compared to rest periods after LE videos (Fig. 2). We computed connectivity matrices using Pearson correlations between the time-series of every pair of nodes in the three networks of interest. The resulting connectivity matrices obtained for each participant were then group-averaged for illustration (see supplementary Fig. 3). In both experiments, we observed a general pattern of intra-network connectivity (Empa-Empa, Amy-Amy, DMN-DMN) during rest periods subsequent to both the HE and LE videos (see supplementary Fig. 3), consistent with functionally coherent activity within each specific network. To specifically unravel the differential connectivity during rest periods due to emotional inertia (post HE vs post LE rest periods), we directly compared the two connectivity matrices using permutation tests (see methods).

In Experiment 1, significant differences were observed for functional connections of the DMN with bilateral amygdala selectively in older adults: In contrast to post-LE rest periods, resting after HE videos exhibited stronger coupling between the PCC and right amygdala *(t* = 2.52, *P* = 0.008, *Z* = 2.4 one-tailed), PCC and left amygdala *(t* = 2.1, *P* = 0.02, *Z* = 1.97 one-tailed), as well as between the aMPFC and right amygdala *(t* = 2.02, *P* = 0.03, *Z* = 1.95 one-tailed), and between aMPFC and left amygdala *(t* = 2.24, *P* = 0.02, *Z* = 2.04 one-tailed) (Fig. 7a). No significant differences in functional connectivity between rest periods after HE and LE videos were found for young adults (see Fig. 7a).

To confirm these age-related differences in functional connectivity patterns, we performed *t*-tests for each connectivity node between younger and older adults. This direct between-group comparison (Young vs Old: Rest post HE > post LE) showed that, in contrast to younger adults, the older showed significantly larger increases in connectivity between left amygdala and PCC (*t* = 2.12, *P* = 0.03, two-tailed), as well as left amygdala and aMPFC(*t* = 2.08, *P* = 0.04, two-tailed) (Fig. 7b).

Experiment 2 revealed similar patterns of increased connectivity in our larger group of elderly. Significant differences were observed for highly selective functional connections of the DMN with limbic areas: In contrast to rest periods after LE videos, rest periods after HE videos induced stronger functional coupling between the PCC and the right amygdala *(t* = 1.82, *P* = 0.03, *Z* = 1.81 one-tailed), as well as between the aMPFC and left insula (*t* = 1.98, *P* = 0.02, *Z* = 2.02 one-tailed). In addition, there was also higher coupling of the bilateral amygdala during rest periods after HE vs LE videos (right with left, *t* = 1.88, *P* = 0.02, *Z* = 1.95 one-tailed) (Fig. 7c).

Because r.AMYG-PCC functional connectivity during rest post HE > LE was significantly increased in older adults from Experiment 1 and this results was replicated in older adults from Experiment 2, we conducted additional *t*-tests in Experiment 2 that allowed us to assess whether the between-network functional coupling for this pair of nodes was also statistically stronger than for other pairs of nodes including either the right amygdala or the PCC. Results showed that r.AMYG-PCC connectivity was indeed significantly greater than between-network connectivity for other pairs of nodes including left AI-PCC, right AI-PCC and right AMYG-aMPFC (see Fig. 8a).

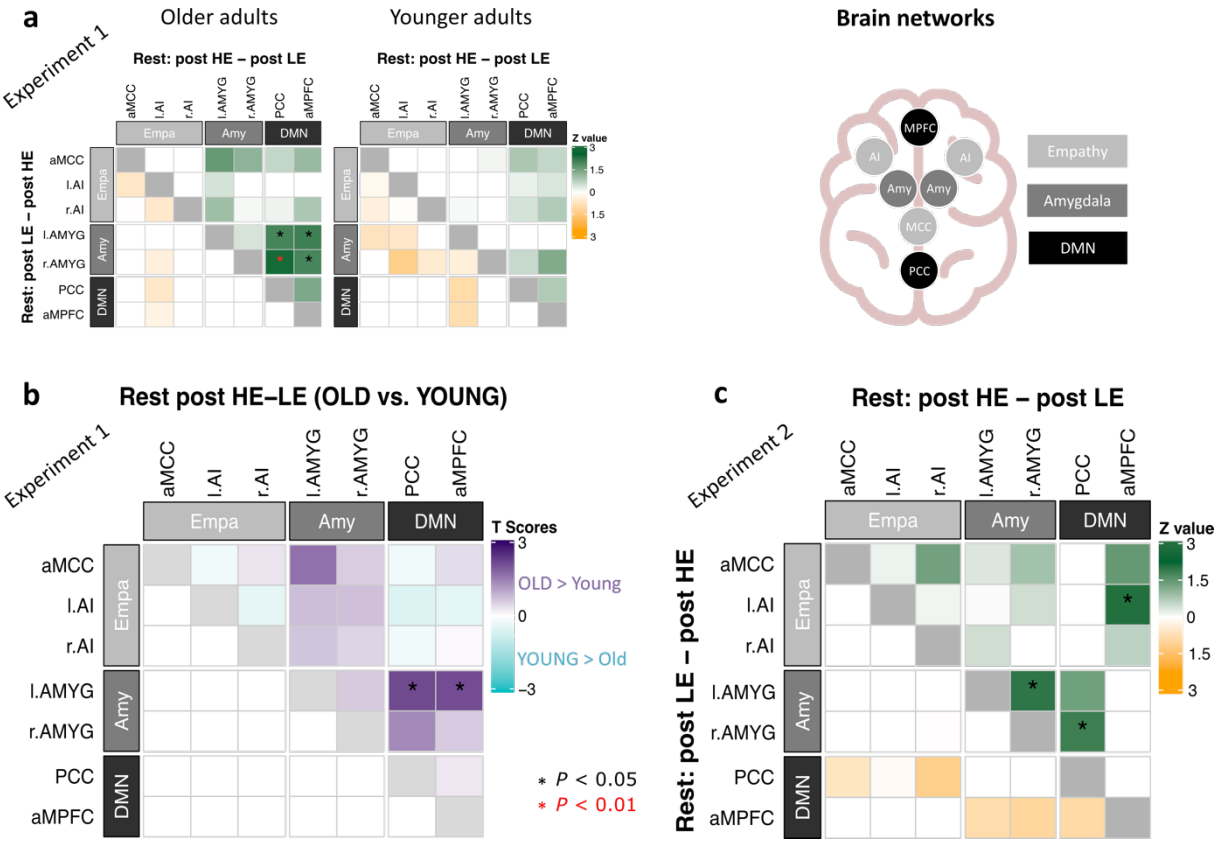

Figure 7. Functional connectivity (FC) results illustrated as correlation matrices between pairs of ROIs for the different rest conditions in Experiment 1 (a,c) and Experiment 2 (d). **a** Correlation for the difference between the two rest conditions, showing functional coupling between regions for post emotion increases (green) and post emotion decreases (orange) for each age group in Experiment 1, N=55). Left and right halves of the matrix with respect to the diagonal depict the values for inverse contrasts (upper part: post HE - post LE rest periods; lower part: post LE - post HE rest periods. Significant changes in correlations with $Z > 1.64$ are marked by an asterisk * corresponding to $P < 0.05$, one-tailed). **b** Age-related differences between functional connectivity changes (Rest post HE > post LE: Old vs Young) were examined with two sample *t*-tests to identify increases predominating in older adults (OLD > YOUNG, violet) or younger adults (YOUNG > OLD, blue). Significant differences were observed only for older relative to younger aduls, depicted by an asterix * corresponding to $P < 0.05$, two-tailed, uncorrected. **c** Correlation matrix showing significant differences in FC between rest conditions in older adults (N=127) from Experiment 2. The upper right figure illustrates the a priori ROIs selected for the current analysis, including regions from the default mode network, DMN (PCC: posterior cingulate cortex, aMPFC: anterior medial prefrontal cortex.), empathy network, Empa (left and right AI: anterior insula, MCC: anterior mid-cingulate cortex) and bilateral amygdalae, Amy (left and right AMYG).

Relationship between functional connectivity patterns and psycho-affective measures

Our fMRI connectivity analyses identified a selective impact of emotional videos on functional brain connectivity of the posterior DMN (PCC) with the amygdala, replicated across two independent experiments carried out at different sites. In Experiment 1, connectivity at rest was significantly increased between PCC and bilateral amygdalae in older adults as well as between PCC and left amygdala when directly comparing older to younger adults. In Experiment 2, connectivity was significantly increased between PCC and right amygdala in the larger older sample. These converging results provide a plausible neural mechanism underlying emotional inertia [16,24] that is specific to older adults and may thus offer a valuable biomarker of homestatic emotion regulation processes in aging.

In Experiment 2, we could therefore further examine whether this connectivity pattern was related to individual differences in socio-emotional abililites and psycho-affective traits. To do so, we tested for a correlation between the *Z*-values from significant edges in connectivity matrices (i.e., connections between two ROIs showing a significant difference $Z > 1.64$ between post HE vs post LE rest) and specific scores on trait anxiety (STAI-trait), rumination (RRS), and empathy (IRI). This analysis showed a significant positive relationship between the magnitude of changes in r.AMYG-PCC connectivity (rest HE – rest LE) and the individual scores of trait anxiety ($r = 0.21$, $P < 0.01$, two-tailed) and rumination ($rho = 0.22$, $P < 0.01$, two-tailed) (Fig. 8b), but no correlation with empathy ($r = 0.1$, $P = 0.25$, two-tailed).

Relationship between functional connectivity patterns and thought probes

Because we observed that rumination scores were positively associated with greater changes in functional coupling between r.AMYG-PCC for the contrast post HE > post LE at rest, we reasoned that some participants (i.e., with higher ruminative tendencies) may have kept more negative-related content in their thoughts during the rest periods after emotional videos. This was directly tested in Experiment 2 by using the explicit thought probe given after different rest conditions (see Fig. 1b). To do so, we compared the r.AMYG-PCC connectivity between a subgroup of participants who verbally reported negative content in their spontaneous

thoughts in response to the probe question (Present) vs. those who did not (Absent), for both the HE and LE conditions.

Behaviorally, for rest periods after HE videos, 59(54%) participants reported negative thought content, while 30(28%) reported no negative thought content and 20(18%) were ambiguous (judgments by our two raters did not match). Interrater reliability analyses revealed a good agreement (kappa=0.61) between the two independent raters (see supplementary Table 4 for details). A Chi-square test revealed that these proportions (negative present 54% vs. negative absent 28%) were statistically different; X^2 (1, N = 109) = 45.88, $P < 0.001$ (two-tailed), demonstrating that HE videos induced more frequent negative than non-negative thoughts in our participants.

Conversely, for rest periods after LE videos, only 41(37%) participants reported negative thought content, while 50(45%) reported no negative thoughts, and 19 (17%) were considered ambiguous. The rater agreement was again good (kappa = 0.66) (see supplementary Table 4 for details). This proportion of negative thoughts (37%) was significantly lower than the proportion of non-negative thoughts (45%); Chi-squared test, X^2 (1, N = 110) = 51.59, $P < 0.001$ (two-tailed), indicating that the LE videos induced less frequent negative mental thought content (than non-negative thoughts). An additional McNemar's test further determined that, as expected, participants reported more negative thoughts for rest periods after HE videos than for rest periods after LE videos, X^2 = 10.28, P = 0.02 (two-tailed).

Finally, to relate these behavioral indices to brain effects, we used a non-parametric permutation analysis in which the r.AMYG-PCC connectivity difference (*observed diff* = 0.08) between these two subgroups (negative thoughts Present-Absent) was compared to a null-distribution built by permuting the labels 5000 times. As hypothesized, we found that the 54% of participants reporting negative content in their thoughts (vs. 28% not reporting) showed increased r.AMYG-PCC connectivity for the rest periods following HE videos (P = 0.02, one-tailed). The same difference between the two subgroups for rest periods following LE videos was only a trend (*observed diff* = 0.06; P = 0.07, one-tailed) (Fig. 8c). Taken together, these findings further unveil a direct relation between r.AMYG-PCC connectivity changes after negative emotions and individual reactivity to aversive or stressful socio-emotional stimuli.

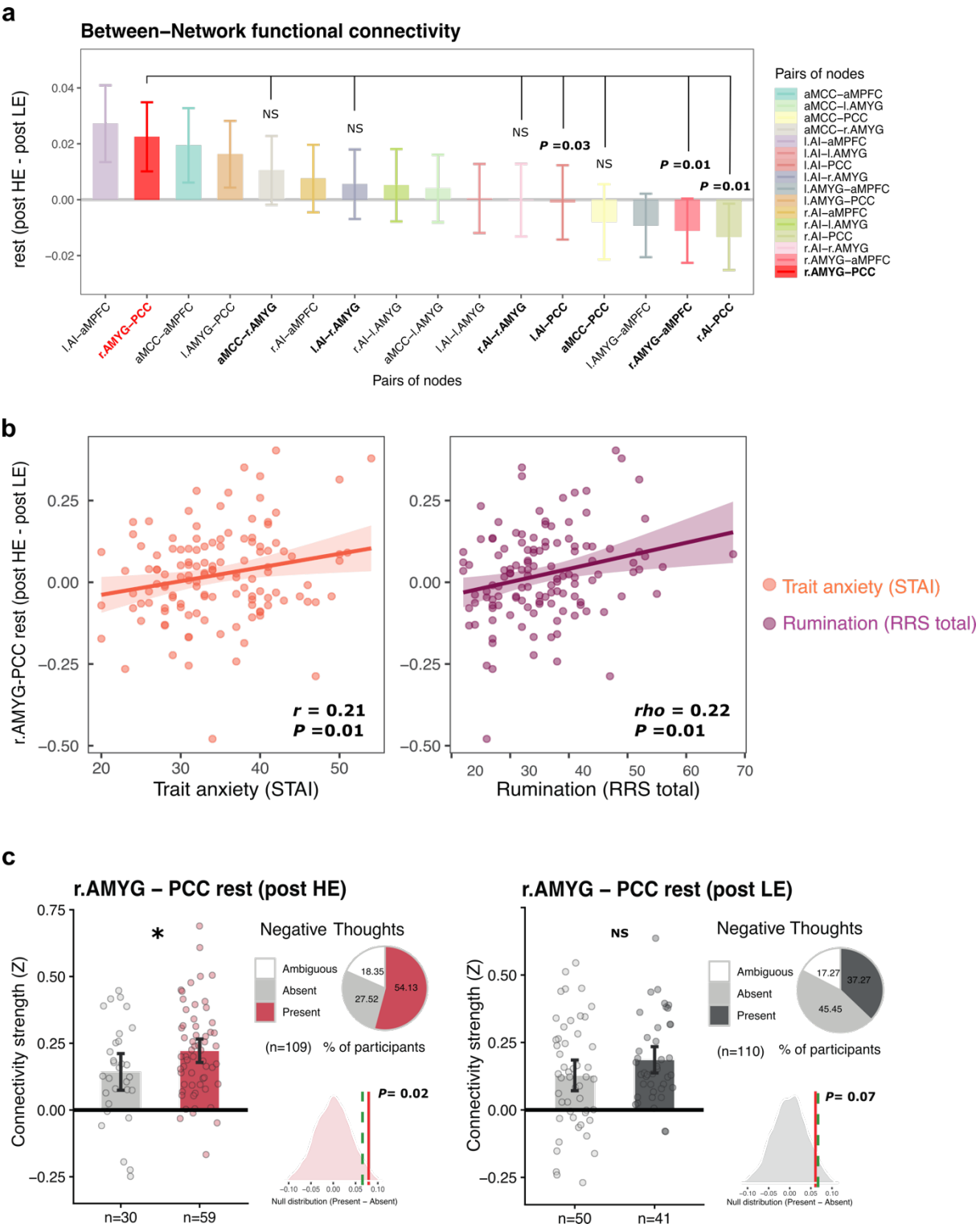

Figure 8. (**a**) Between-network functional connectivity during rest periods after HE > LE videos. Pairs of nodes are ordered from left to right according to the connectivity strenght. In red, the r.AMYG-PCC pair was significantly more connected than other pairs (but not all) involving either the PCC or the right amygdala (in bold); significant comparisons from *t*-tests (one-tailed) are marked with corresponding *P* values, NS: not significant (**b**)Pearson (*r*) and Spearman (*rho*) correlations show that higher functional connectivity between amygdala and posterior cingulate cortex during rest periods after HE > LE videos [r.AMYG-PCC(rest HE-rest LE)] was positively related to trait anxiety (STAI.B) and rumination (RRS total). (**c**) r.AMYG-PCC connectivity between the group of participants who verbally reported negative content during the thought probes (Present) vs. the group who did not (Absent), for both HE and LE conditions. After HE videos, 59(54%) participants reported

negative content in their thought probes, 30(28%) did not report negative content and 20(18%) were ambiguous. After LE videos, only 41(37%) reported negative content, 50(45)% reported negative thoughts, and 19(17%) were ambiguous. At the brain level, we performed a non-parametric permutation analysis to compare the observed mean r.AMYG-PCC connectivity difference between the two groups Present-Absent (*observed diff* = 0.08), relative to a null-distribution built by permuting the labels 5000 times. As hypothesized, we found that 54% of the participants reporting negative content in their thoughts (vs. 28% not reporting negative thoughts) showed increased r.AMYG-PCC connectivity in the HE condition (P = 0.02, one-tailed). In the LE condition, there was no significant difference in r.AMYG-PCC connectivity between the two groups (*observed diff* = 0.06; P = 0.07, one-tailed). Red: High Emotion (HE) condition, Grey: Low emotion (LE) condition. r.AMYG-PCC: connectivity between the right amygdala and the posterior cingulate cortex. Percentages in the text are rounded. Data from Experiment 2.

DISCUSSION

The current study sought to delineate neural markers of emotional resilience and empathy in aging, which are increasingly recognized as important protective factors against mental illness and cognitive decline in this population [80]. We assessed both reactivity and recovery of brain networks to negative socio-affective situations (i.e., during and after videos) in two independent experiments, including a large number of younger and older adults (N=182). In Experiment 1, we focused on validating the task and assessing aging effects on affective processes that allowed us to probe for emotional carryover effects in resting state (emotional inertia) as an indirect indicator of maladaptive regulation processes [16]. In Experiment 2, we replicated the results and further examined the relationship between brain carryover effects and measures of anxiety, rumination, and negative thoughts in older adults.

Aging effects on behavioral characteristics

Overall, our two samples of older adults (Experiment 1 and Experiment 2) did not differ in any of the questionnaires assessing affective or cognitive traits. Compared to younger adults, older adults reported lower scores in cognitive-related processes, including reflective rumination and cognitive empathy. These findings converge with previous work showing a decline of cognitive abilities as people get older, including cognitive components of social functions [4], while socio-affective abilities tend to remain stable.

Accordingly, measures of affect and empathy showed largely preserved patterns in the elderly that extend previous findings in younger adults [55]. Seeing videos of others' suffering

induced higher levels of negative affect, lower positive affect, and higher empathy scores than mundane scenes of daily life, in both younger and older participants. Nonetheless, age differences were observed, with older adults reporting more positive emotions for both LE and HE videos. Moreover, despite a restricted age range in our elderly population, we found that the older the age, the lower the negative and the higher the positive emotions reported to videos of suffering (see Fig. 4b). This relationship between age and affect was not present for young participants. These results confirm the "positivity bias" often described in the elderly [7], which may reflect a motivation to upregulate positive and downregulate negative information from emotional stimuli [7]. In contrast, young and older adults reported similar levels of negative affect in response to others' suffering. This suggests that the positivity bias of older adults does not necessarily impair their capacity to feel negative emotions when facing someone who is suffering. This underlines the importance of separately assessing negative and positive emotions, as done in the SoVT-Rest task, an issue already highlighted in previous research[81,82]

Finally, we found that emotional responses were modulated by levels of experienced empathy. Higher empathy correlated not only with increased negative affect during HE videos but also with increased positive affect during LE videos, for both older and younger adults (see Fig. 4c). However, positive emotions were reduced with higher empathy during HE videos only in older adults. These results indicate that modulation of positive emotions by empathy in older adults may depend on the context: the higher the empathy, the higher the positive emotions when facing social stimuli without overt emotional content, but the lower the positive emotions when facing social stimuli of others' distress. These data offer a new perspective on how empathy for others' suffering may impact the "positivity bias" usually observed in the elderly.

Brain activity markers of empathy and age differences

Exposure to others' suffering (contrast HE > LE videos) engaged several regions overlapping with networks previously associated with social cognition and emotion. These encompassed regions related to affective empathy, pain processing, or more generally salience detection (aMCC, AI), as well as parts of the theory of mind (ToM) network (PCC, r.TPJ, dMPFC, IFG) and the compassion network (ventral striatum) [77,79]. These results converge with abundant evidence implicating aMCC and AI in empathy for pain [36,50], encoding behaviorally

salient information [83,84] and negative affect [85,86]. Likewise, TPJ and dMPFC are consistently engaged in scenarios requiring cognitive abilities to infer others' affective and mental state [87,88], and therefore implicated in cognitive aspects of empathy and theory of mind [36,51]. In addition, in younger adults in Experiment 1 and the larger sample of older adults in Experiment 2, the HE>LE videos also activated clusters in ventral striatum, an area associated with positive affect and reward [89] and engaged during compassion for other's suffering [64,77].

Remarkably, despite its prominent role in emotional processing, there was no significant activation in the amygdala during the HE > LE videos in either group. This null result might however accord with the notion that the amygdala responds more broadly to social or self-relevant information rather than just negative valence [90,91], and may already activate to the content of LE videos. This would accord with similar increases seen during both video conditions in Experiment 2 (see supplementary Fig. 2 and Fig. 6h).

Importantly, age differences were observed in these neural responses. Older adults activated less regions typically related to empathy (AI, PAG) and more those related to social cognition and emotion regulation (DMPFC, PCC, IFG). This adds to a few previous studies that examined age-effects on empathy for pain [43,46] and empathy for negative and positive emotions [92]. Lower activity in affect-related regions, along with higher activity in cognition-related frontal regions have been interpreted as a mechanism for enhanced emotion regulation perfomance, possibly mediating the positivity bias of older people [3,93]. On the other hand, increased activity in frontal regions may also reflect compensatory brain mechanisms acting to overcome cognitive deterioration in older adults (Cabeza, 2002; Davis, 2008). Further research is therefore needed to explicitely test cognitive functioning and clarify how it accounts for this activation pattern in older adults, an issue beyond the purpose of the present study.

In any case, our findings suggest that socio-affective functions and brain regions mediating empathy and theory of mind exhibit globally normal patterns of engagement in response to negative social situations in the healthy elderly. These data also demonstrate that our video paradigm effectively engaged emotion and empathy processes in our participants, and confirm a positive affective bias of older individuals in both their behavioral and neural responses to social scenes, indicating globally preserved empathy and emotional balance.

Emotional inertia and recovery from emotions after exposure to others' suffering

Beyond transient responses to negative stimuli, assessing the impact of emotions over time is crucial to determine how people cope with stressful events [94]. Emotional inertia denotes a persistence of emotional states [16] reflecting inefficient recovery and greater risk for psychological maladjustment [22,94–96]. Although well-studied behaviorally [16,20], emotional inertia remains largely unexplored at the brain level, especially in old populations. To uncover its neural underpinnings, we probed for carryover effects in brain activity at rest following exposure to emotional videos and assessed age-related differences.

Across our two experiments, we observed selective increases during rest periods after HE relative to LE videos in midline brain areas (ACC/MPFC and Precuneus/PCC), involving core parts of the DMN typically active at rest [72], together with increases in amygdala and insula, two regions implicated in emotional processing [37]. Importantly, these effects occurred only in older adults, suggesting an important modulation of emotion regulation mechanisms during aging. The DMN is implicated in self-related internally-oriented processes, including memory, interoception, and value-based decision making [33,34]. Interestingly, previous research found that the duration of activation in midline DMN regions was a better predictor of the subjective emotional intensity of negative stimuli than the magnitude of activation [26]. Other fMRI studies reported modulations of DMN in response to emotional challenges, although with divergent findings. While some researchers reported attenuated DMN activation following various emotions [24,25], others reported increases [26,32], similar to the current results. In Experiment 2, we further found that two midline nodes of DMN (i.e., Precuneus/PCC and dMPFC) were not only activated in the HE > LE contrast during videos, but also continued their activity in the corresponding contrast during subsequent rest (post HE > post LE), providing direct evidence for "emotional inertia" in the aging brain. These findings resonate with previous work showing that older, but not younger, adults fail to deactivate regions of the DMN during cognitive control and visuospatial tasks [41,42]. To our knowledge, these data reveal for the first time that increased DMN activations in the elderly can persist over time after exposure to negative socio-emotional contexts.

Sustained changes were also observed in limbic regions in Experiment 2. The anterior insula showed increased activity during both the (HE > LE) videos and the (post HE > post LE) rest periods, although the voxelwise activations did not fully overlap between the two conditions: while there was a more dorsal engagement during videos, more ventral parts of

981 the anterior insula were active after the emotional event. In light of previous research in
982 younger adults [97] suggesting that dorsal AI may be recruited during adaptive behavior
983 mechanisms while ventral AI may be highly recruited during internal homeostatic regulation,
984 our result may reflect a shift from controlled/explicit adaptation to more spontaneous/implicit
985 homeostatic regulation. On the other hand, the amygdala did not differentially respond during
986 the (HE > LE) videos, but it showed a lower return to baseline levels during rest after HE vs.
987 LE videos. Accordingly, prolonged amygdala activity after negative images was reported to
988 predict greater trait neuroticism [38], and enhanced amygdala response to threat faces after
989 negative emotion elicitation is amplified in high anxiety individuals [19].
990 Altogether, our data highlight the importance of the temporal dynamics of brain
991 responses to emotion in order to determine individual affective styles and risks for
992 psychopathology [24,26,29].
993

Brain connectivity patterns related to emotional inertia

Our functional connectivity analysis revealed that post-emotional carryover effects were organized in different circuits, linking core parts of the DMN (PCC and MPFC) with limbic regions (amygdala and anterior insula). These connections were selectively enhanced in post HE relative to post LE rest, exclusively in older adults, and across both experiments (see Fig. 7). These results unveil sustained coupling patterns between the midline DMN and limbic networks induced by emotional inertia, which were accompanied by distinctive behavioral features.

The PCC and amygdala were more active and functionally more connected in the post-emotional rest periods in older adults. Detailed analyses of Experiment 2 revealed that PCC-amygdala connectivity was stronger for HE than LE conditions, but also selectively stronger than other between-network connectivity patterns involving either the PCC or the amygdala (see Fig. 8a). Interestingly, the strength of PCC-amygdala enhanced connectivity was predicted by individual anxiety and rumination. Older adults reporting higher rumination tendencies and anxious traits on questionnaires also exhibited stronger PCC-amygdala connectivity after emotional videos. In addition, explicit verbal reports revealed that more participants expressed negative thought contents during the rest period that followed HE videos. Importantly, these participants with more frequent negative thoughts also had higher PCC-amygdala connectivity than those who reported no negative thoughts, and this was not the case during rest periods after LE videos. These findings suggest that increased functional connectivity between PCC and amygdala may directly underpin the persistence of negative content in spontaneous thoughts.

Past neuroimaging research suggests that PCC is involved in internally directed cognition, rumination and memory [34,98] especially when people retrieve contextual and affective autobiographical information [99,100]. As the amygdala also plays a central role in affective memory by encoding and storing information about emotional relevance [35,90,101], we speculate that PCC-amygdala communication may contribute to emotional inertia and recovery from socio-emotional stressful situations, possibly by associating the content of vicarious negative experiences to personal affective memories in older adults, and especially in individuals with higher levels of anxiety and rumination. These data unveil new age-related effects on neural processes associated with rumination and repetitive negative thinking, i.e.,

mental states implying persistent self-relevant thoughts about negative information [102] that are associated not only with maladaptive emotion regulation but also with increased risk of cognitive decline and Alzheimer's disease [12,14]. As neurodegenerative anomalies in PCC and medial brain regions are commonly seen in Alzheimer's disease [103,104], changes in PCC connectivity might constitute a possible neural marker for deficient affective resilience, which is in turn associated with a higher risk for dementia.

Our results thus complement prior work on DMN connectivity in aging populations. Indeed, recent research demonstrated that functional connectivity between the DMN and cognitive control regions (dlPFC) was modulated by the cognitive load/efforts on the task in older but not younger adults [42]. Our data extend this to affective contexts and link it to speficic psychological traits. Indeed, DMN connectivity to limbic regions is amplified after emotional induction in older (but not younger) adults, with PCC-amygdala coupling being distinctively sensitive to anxiety, rumination, and self-reports of negative thoughts.

In parallel, increased functional connectivity was also observed between AI and aMPFC after HE compared to LE videos in the larger older adult sample from Experiment 2. These neural changes showed no correlation with anxiety or rumination but only a weak positive correlation with the empathic concern IRI subscale (see supplementary Fig. 4). These findings may reflect a more general role of AI in emotional awareness [105,106] and empathy [36], and of aMPFC in the representation of affective states in both the self and others [78,107]. These results extend prior work by showing that modulation of connectivity between these two regions may occur not only during the appraisal of socio-emotional stimuli but also persist beyond emotional events.

LIMITATIONS AND FUTURE DIRECTIONS

Some limitations of our study need to be acknowledged. First, we explicitly instructed participants to watch videos passively, and therefore some of the subsequent carryover effects on brain activity and connectivity could be interpreted as unsuccessful implicit emotion regulation styles inherent to the participants. It would be interesting to assess in future studies whether instructing participants with explicit emotion regulation strategies may change the subsequent brain response related to emotional inertia. Second, technical constraints of the fMRI scanner also engendered some limitations. First, as explained in the methods, we

obtained affective ratings on videos outside of the scanner, immediately after the scanning session. Although this may bias how participants rated the videos, we deliberately made the choice in order to 1) avoid top-down cognitive influences during scanning which may confound neural activity during emotional perception [65,66]; and 2) maximize older adults' comfort by reducing the time spent inside the scanner (particularly because other anatomical and functional MRI sequences including T1, T2 and T2* were carried out during the same session). Second, as described in supplementary Fig. 5, some basal forebrain voxels were automatically excluded from our group analyses in Experiment 2, due to magnetic field inhomogeneities frequently induced in brain regions near air-filled cavities in the human head [108]. Consequently, we were not able to reliably study regions such as the orbitofrontal cortex (OFC), which plays an essential role in positive emotions and reward [64,89].

CONCLUSION

In sum, our study demonstrates that empathy for suffering and affective resilience can reliably be investigated in the elderly using the SoVT-Rest, a novel paradigm that has very low cognitive load and high ecological validity for applications in frail or clinical populations. Using the SoVT-Rest, we find neural and behavioral markers of the positivity bias in the elderly and show for the first time sustained carryover effects (or emotional inertia) in corticolimbic brain circuits in populations of healthy older adults. Interestingly, PCC and amygdala's functional connectivity at rest was increased during high emotional events, and such increase was related to anxiety, rumination, and negative thought content, making this resting connectivity pattern a highly likely neural substrate for emotional inertia. These findings provide an important cornerstone for better understanding empathy and mechanisms underlying affective resilience in the brain of the elderly population, and thus contribute to identifying potential risk markers for neurodegenerative diseases associated with poor social stress coping.

DATA AVAILABILITY

The data underlying this report are made available on request following a formal data sharing agreement and approval by the consortium and executive committee (https://silversantestudy.eu/2020/09/25/data-sharing). The Material can be mobilized, under the conditions and modalities defined in the Medit-Ageing Charter, by any research team

belonging to an Academic for carrying out a scientific research project relating to the scientific theme of mental health and well-being in older people. The Material may also be mobilized by non-academic third parties, under conditions, in particular financial, which will be established by separate agreement between Inserm and by the said third party. Data sharing policies described in the Medit-Ageing Charter are in compliance with our ethics approval and guidelines from our funding body.

CODE AVAILABILITY

The code used to produce the results reported in the manuscript can be made available upon appropriate request.

REFERENCES

1. Glisky, E. Changes in Cognitive Function in Human Aging. 3–20 (2007). doi:10.1201/9781420005523.sec1
2. Carstensen, L. L., Mayr, U., Pasupathi, M. & Nesselroade, J. R. Emotional experience in everyday life across the adult life span. *J. Pers. Soc. Psychol.* **79**, 644–655 (2000).
3. Mather, M. The Affective Neuroscience of Aging. (2015). doi:10.1146/annurev-psych-122414-033540
4. Reiter, A. M. F., Kanske, P., Eppinger, B. & Li, S.-C. The Aging of the Social Mind - Differential Effects on Components of Social Understanding. *Sci. Rep.* **7**, 11046 (2017).
5. Urry, H. L. & Gross, J. J. Emotion regulation in older age. *Curr. Dir. Psychol. Sci.* **19**, 352–357 (2010).
6. Lang, F. R. & Carstensen, L. L. Time counts: Future time perspective, goals, and social relationships. *Psychol. Aging* **17**, 125–139 (2002).
7. Mather, M. & Carstensen, L. L. Aging and motivated cognition: The positivity effect in attention and memory. *Trends in Cognitive Sciences* **9**, 496–502 (2005).
8. Aldao, A., Nolen-Hoeksema, S. & Schweizer, S. Emotion-regulation strategies across psychopathology: A meta-analytic review. *Clin. Psychol. Rev.* **30**, 217–237 (2010).
9. Hamilton, J. P., Farmer, M., Fogelman, P. & Gotlib, I. H. Depressive Rumination, the Default-Mode Network, and the Dark Matter of Clinical Neuroscience. *Biol. Psychiatry* **78**, 224–230 (2015).
10. Kraaij, V., Pruymboom, E. & Garnefski, N. Cognitive coping and depressive symptoms in the elderly: A longitudinal study. *Aging Ment. Heal.* **6**, 275–281 (2002).
11. Terracciano, A. *et al.* Personality and risk of Alzheimer's disease: New data and meta-analysis. *Alzheimer's Dement.* **10**, 179–186 (2014).
12. Marchant, N. L. & Howard, R. J. Cognitive debt and Alzheimer's disease. *J. Alzheimer's Dis.* **44**, 755–770 (2015).
13. Wilson, R. S., Begeny, C. T., Boyle, P. A., Schneider, J. A. & Bennett, D. A. Vulnerability to Stress, Anxiety, and Development of Dementia in Old Age. *Am. J. Geriatr. Psychiatry* **19**, 327–334 (2011).

14. Marchant, N. L. *et al.* Repetitive negative thinking is associated with amyloid, tau, and cognitive decline. *Alzheimer's Dement.* 1–11 (2020). doi:10.1002/alz.12116
15. Jané-Llopis, E. *et al. Mental Health in Older People*. (2008).
16. Kuppens, P., Allen, N. B. & Sheeber, L. B. Emotional inertia and psychological maladjustment. *Psychol. Sci.* **21**, 984–991 (2010).
17. Koval, P., Kuppens, P., Allen, N. B. & Sheeber, L. Getting stuck in depression: The roles of rumination and emotional inertia. *Cogn. Emot.* **26**, 1412–1427 (2012).
18. Van De Leemput, I. A. *et al.* Critical slowing down as early warning for the onset and termination of depression. *Proc. Natl. Acad. Sci. U. S. A.* **111**, 87–92 (2014).
19. Pichon, S., Miendlarzewska, E. A., Eryilmaz, H. & Vuilleumier, P. Cumulative activation during positive and negative events and state anxiety predicts subsequent inertia of amygdala reactivity. *Soc. Cogn. Affect. Neurosci.* **10**, 180–190 (2015).
20. Suls, J., Green, P. & Hillis, S. Emotional reactivity to everyday problems, affective inertia, and neuroticism. *Personal. Soc. Psychol. Bull.* (1998). doi:10.1177/0146167298242002
21. Koval, P., Pe, M. L., Meers, K. & Kuppens, P. Affect dynamics in relation to depressive symptoms: Variable, unstable or inert? *Emotion* **13**, 1132–1141 (2013).
22. Trull, T. J., Lane, S. P., Koval, P. & Ebner-Priemer, U. W. Affective Dynamics in Psychopathology. *Emot. Rev.* **7**, 355–361 (2015).
23. Lamke, J. P. *et al.* The impact of stimulus valence and emotion regulation on sustained brain activation: Task-rest switching in emotion. *PLoS One* **9**, (2014).
24. Eryilmaz, H., Van De Ville, D., Schwartz, S. & Vuilleumier, P. Impact of transient emotions on functional connectivity during subsequent resting state: A wavelet correlation approach. *Neuroimage* **54**, 2481–2491 (2011).
25. Pitroda, S., Angstadt, M., McCloskey, M. S., Coccaro, E. F. & Phan, K. L. Emotional experience modulates brain activity during fixation periods between tasks. *Neurosci. Lett.* **443**, 72–76 (2008).
26. Waugh, C. E., Hamilton, J. P. & Gotlib, I. H. The neural temporal dynamics of the intensity of emotional experience. *Neuroimage* **49**, 1699–1707 (2010).
27. Veer, I. M. *et al.* Beyond acute social stress: Increased functional connectivity between amygdala and cortical midline structures. *Neuroimage* **57**, 1534–1541 (2011).
28. Eryilmaz, H., Van De Ville, D., Schwartz, S. & Vuilleumier, P. Lasting impact of regret and gratification on resting brain activity and its relation to depressive traits. *J. Neurosci.* **34**, 7825–7835 (2014).
29. Waugh, C. E., Hamilton, J. P., Chen, M. C., Joormann, J. & Gotlib, I. H. Neural temporal dynamics of stress in comorbid major depressive disorder and social anxiety disorder. *Biol. Mood Anxiety Disord.* **2**, 1–15 (2012).
30. Northoff, G., Qin, P. & Nakao, T. Rest-stimulus interaction in the brain: A review. *Trends Neurosci.* **33**, 277–284 (2010).
31. Gaviria, J., Rey, G., Bolton, T., Van De Ville, D. & Vuilleumier, P. Dynamic functional brain networks underlying the temporal inertia of negative emotions. *Neuroimage* **240**, 118377 (2021).
32. Schneider, F. *et al.* The resting brain and our self: Self-relatedness modulates resting state neural activity in cortical midline structures. *Neuroscience* **157**, 120–131 (2008).
33. Raichle, M. E. *et al.* A default mode of brain function. *Proc. Natl. Acad. Sci.* (2001). doi:10.1073/pnas.98.2.676
34. Buckner, R. L., Andrews-Hanna, J. R. & Schacter, D. L. The brain's default network: Anatomy, function, and relevance to disease. *Ann. N. Y. Acad. Sci.* **1124**, 1–38 (2008).
35. LeDoux, J. The emotional brain, fear, and the amygdala. *Cellular and Molecular Neurobiology* (2003). doi:10.1023/A:1025048802629

36. Lamm, C., Decety, J. & Singer, T. Meta-analytic evidence for common and distinct neural networks associated with directly experienced pain and empathy for pain. *Neuroimage* **54**, 2492–2502 (2011).
37. Meaux, E. & Vuilleumier, P. *Emotion Perception and Elicitation*. *Brain Mapping: An Encyclopedic Reference* **3**, (Elsevier Inc., 2015).
38. Schuyler, B. S. *et al.* Temporal dynamics of emotional responding: Amygdala recovery predicts emotional traits. *Soc. Cogn. Affect. Neurosci.* **9**, 176–181 (2014).
39. Kim, M. J. *et al.* The structural and functional connectivity of the amygdala: From normal emotion to pathological anxiety. *Behav. Brain Res.* **223**, 403–410 (2011).
40. Rey, G. *et al.* Resting-state functional connectivity of emotion regulation networks in euthymic and non-euthymic bipolar disorder patients. *Eur. Psychiatry* **34**, 56–63 (2016).
41. Spreng, R. N. & Schacter, D. L. Default Network Modulation and Large-Scale Network Interactivity in Healthy Young and Old Adults. *Cereb. Cortex* **22**, 2610–2621 (2012).
42. Turner, G. R. & Spreng, R. N. Prefrontal Engagement and Reduced Default Network Suppression Co-occur and Are Dynamically Coupled in older Adults: The Default-Executive Coupling Hypothesis of Aging. *J. Cogn. Neurosci.* **27**, 2462–2476 (2015).
43. Chen, Y.-C., Chen, C.-C., Decety, J. & Cheng, Y. Aging is associated with changes in the neural circuits underlying empathy. *Neurobiol. Aging* **35**, 827–836 (2014).
44. Hühnel, I., Fölster, M., Werheid, K. & Hess, U. Empathic reactions of younger and older adults: No age related decline in affective responding. *J. Exp. Soc. Psychol.* **50**, 136–143 (2014).
45. Moore, R. C., Dev, S. I., Jeste, D. V., Dziobek, I. & Eyler, L. T. Distinct neural correlates of emotional and cognitive empathy in older adults. *Psychiatry Res. - Neuroimaging* **232**, 42–50 (2015).
46. Tamm, S. *et al.* The effect of sleep restriction on empathy for pain: An fMRI study in younger and older adults. *Sci. Rep.* **7**, 1–14 (2017).
47. Beadle, J. N. & De La Vega, C. E. Impact of aging on empathy: Review of psychological and neural mechanisms. *Front. Psychiatry* **10**, 1–13 (2019).
48. Sze, J. A., Gyurak, A., Goodkind, M. S. & Levenson, R. W. Greater emotional empathy and prosocial behavior in late life. *Emotion* **12**, 1129–1140 (2012).
49. Bailey, P. E., Brady, B., Ebner, N. C. & Ruffman, T. Effects of age on emotion regulation, emotional empathy, and prosocial behavior. *Journals Gerontol. - Ser. B Psychol. Sci. Soc. Sci.* **75**, 802–810 (2020).
50. Fan, Y., Duncan, N. W., de Greck, M. & Northoff, G. Is there a core neural network in empathy? An fMRI based quantitative meta-analysis. *Neurosci. Biobehav. Rev.* **35**, 903–911 (2011).
51. Schurz, M., Radua, J., Aichhorn, M., Richlan, F. & Perner, J. Fractionating theory of mind: A meta-analysis of functional brain imaging studies. *Neurosci. Biobehav. Rev.* **42**, 9–34 (2014).
52. Krueger, K. R. *et al.* Social engagement and cognitive function in old age. *Exp. Aging Res.* **35**, 45–60 (2009).
53. MacLeod, S., Musich, S., Hawkins, K., Alsgaard, K. & Wicker, E. R. The impact of resilience among older adults. *Geriatr. Nurs. (Minneap).* **37**, 266–272 (2016).
54. Zunzunegui, M. V., Alvarado, B. E., Del Ser, T. & Otero, A. Social networks, social integration, and social engagement determine cognitive decline in community-dwelling Spanish older adults. *Journals Gerontol. - Ser. B Psychol. Sci. Soc. Sci.* **58**, (2003).
55. Klimecki, O. M., Leiberg, S., Lamm, C. & Singer, T. Functional neural plasticity and associated changes in positive affect after compassion training. *Cereb. Cortex* **23**,

1552–1561 (2013).
56. Gross, J. J. The emerging field of emotion regulation: An integrative review. *Review of General Psychology* (1998). doi:10.1037/1089-2680.2.3.271
57. Poisnel, G. *et al.* The Age-Well randomized controlled trial of the Medit-Ageing European project: Effect of meditation or foreign language training on brain and mental health in older adults. *Alzheimer's Dement. Transl. Res. Clin. Interv.* **4**, 714–723 (2018).
58. Davis, M. H. & Association, A. P. A multidimensional approach to individual differences in empathy. *JSAS Cat. Sel. Doc. Psychol.* (1980).
59. Sheikh, J. I. & Yesavage, J. A. 9/geriatric depression scale (Gds) recent evidence and development of a shorter version. *Clin. Gerontol.* (1986). doi:10.1300/J018v05n01_09
60. Beck, A. T., Steer, R. A., & Brown, G. K. (1996). BDI-II manual. San Antonio, TX: The Psychological Corporation.
61. Spielberger, C. D., Gorsuch, R. L. & Lushene, R. State-trait anxiety inventory STAI (Form Y). *Redw. City Mind Gard.* (1983). doi:10.1515/9783111677439-035
62. Gross, J. J. & John, O. P. Individual differences in two emotion regulation processes: Implications for affect, relationships, and well-being. *J. Pers. Soc. Psychol.* **85**, 348–362 (2003).
63. Treynore, Gonzalez & Nolen-Hoeksema, S. Ruminative Responses Scale. *Cognit. Ther. Res.* (2003). doi:10.1017/CBO9781107415324.004
64. Klimecki, O. M., Leiberg, S., Ricard, M. & Singer, T. Differential pattern of functional brain plasticity after compassion and empathy training. *Soc. Cogn. Affect. Neurosci.* **9**, 873–879 (2013).
65. Taylor, W. D. *et al.* Smaller orbital frontal cortex volumes associated with functional disability in depressed elders. *Biol. Psychiatry* **53**, 144–149 (2003).
66. Grimm, S. *et al.* Segregated neural representation of distinct emotion dimensions in the prefrontal cortex - An fMRI study. *Neuroimage* **30**, 325–340 (2006).
67. Benjamini, Y. & Hochberg, Y. Controlling the False Discovery Rate: A Practical and Powerful Approach to Multiple Testing. *J. R. Stat. Soc. Ser. B* (1995). doi:10.1111/j.2517-6161.1995.tb02031.x
68. Pruim, R. H. R. *et al.* ICA-AROMA: A robust ICA-based strategy for removing motion artifacts from fMRI data. *Neuroimage* **112**, 267–277 (2015).
69. Villain, N. *et al.* A simple way to improve anatomical mapping of functional brain imaging. *J. Neuroimaging* **20**, 324–333 (2010).
70. Power, J. D., Barnes, K. A., Snyder, A. Z., Schlaggar, B. L. & Petersen, S. E. Spurious but systematic correlations in functional connectivity MRI networks arise from subject motion. *Neuroimage* **59**, 2142–2154 (2012).
71. Lieberman, M. D. & Cunningham, W. A. Type I and Type II error concerns in fMRI research: Re-balancing the scale. *Soc. Cogn. Affect. Neurosci.* **4**, 423–428 (2009).
72. Andrews-Hanna, J. R., Reidler, J. S., Sepulcre, J., Poulin, R. & Buckner, R. L. Functional-Anatomic Fractionation of the Brain's Default Network. *Neuron* **65**, 550–562 (2010).
73. Fair, D. A. *et al.* A method for using blocked and event-related fMRI data to study 'resting state' functional connectivity. *Neuroimage* **35**, 396–405 (2007).
74. Friston, K. J. Functional and effective connectivity in neuroimaging: A synthesis. *Hum. Brain Mapp.* **2**, 56–78 (1994).
75. Winkler, A. M., Ridgway, G. R., Webster, M. A., Smith, S. M. & Nichols, T. E. Permutation inference for the general linear model. *Neuroimage* **92**, 381–397 (2014).
76. Wancata, J., Alexandrowicz, R., Marquart, B., Weiss, M. & Friedrich, F. The criterion validity of the geriatric depression scale: A systematic review. *Acta Psychiatr. Scand.*

114, 398–410 (2006).
77. Singer, T. & Klimecki, O. M. Empathy and compassion. *Curr. Biol.* **24**, R875–R878 (2014).
78. Corradi-Dell'Acqua, C., Hofstetter, C. & Vuilleumier, P. Cognitive and affective theory of mind share the same local patterns of activity in posterior temporal but not medial prefrontal cortex. *Soc. Cogn. Affect. Neurosci.* **9**, 1175–1184 (2014).
79. Preckel, K., Kanske, P. & Singer, T. On the interaction of social affect and cognition: empathy, compassion and theory of mind. *Curr. Opin. Behav. Sci.* **19**, 1–6 (2018).
80. Klimecki, O. M. *et al.* The impact of meditation on healthy ageing — the current state of knowledge and a roadmap to future directions. *Curr. Opin. Psychol.* **28**, 223–228 (2019).
81. Cacioppo, J. T. & Berntson, G. G. Relationship Between Attitudes and Evaluative Space: A Critical Review, With Emphasis on the Separability of Positive and Negative Substrates. *Psychol. Bull.* **115**, 401–423 (1994).
82. Norman, G. J. *et al.* Current emotion research in psychophysiology: The neurobiology of evaluative bivalence. *Emot. Rev.* **3**, 349–359 (2011).
83. Seeley, W. W. *et al.* Dissociable intrinsic connectivity networks for salience processing and executive control. *J. Neurosci.* **27**, 2349–2356 (2007).
84. Menon, V. & Uddin, L. Q. Saliency, switching, attention and control: a network model of insula function. *Brain Struct. Funct.* **214**, 655–667 (2010).
85. Knutson, B., Katovich, K. & Suri, G. Inferring affect from fMRI data. *Trends Cogn. Sci.* **18**, 422–428 (2014).
86. Corradi-Dell'Acqua, C., Tusche, A., Vuilleumier, P. & Singer, T. Cross-modal representations of first-hand and vicarious pain, disgust and fairness in insular and cingulate cortex. *Nat. Commun.* **7**, (2016).
87. Bruneau, E. G., Jacoby, N. & Saxe, R. Empathic control through coordinated interaction of amygdala, theory of mind and extended pain matrix brain regions. *Neuroimage* **114**, 105–119 (2015).
88. Bruneau, E., Dufour, N. & Saxe, R. How We Know It Hurts: Item Analysis of Written Narratives Reveals Distinct Neural Responses to Others' Physical Pain and Emotional Suffering. *PLoS One* **8**, (2013).
89. Knutson, B., Fong, G. W., Adams, C. M., Varner, J. L. & Hommer, D. Dissociation of reward anticipation and outcome with event-related fMRI. *Neuroreport* **12**, 3683–3687 (2001).
90. Sander, D., Grafman, J. & Zalla, T. The Human Amygdala: An Evolved System for Relevance Detection. *Reviews in the Neurosciences* (2003). doi:10.1515/REVNEURO.2003.14.4.303
91. Cunningham, W. A., Raye, C. L. & Johnson, M. K. 0898929042947919. 1–13 (2004).
92. Riva, F. *et al.* Age-related differences in the neural correlates of empathy for pleasant and unpleasant touch in a female sample. *Neurobiol. Aging* **65**, 7–17 (2018).
93. Dolcos, S., Moore, M. & Katsumi, Y. Neuroscience and Well-Being. 1–26 (2018).
94. Davidson, R. J. Affective Style and Affective Disorders: Perspectives from Affective Neuroscience. *Cogn. Emot.* **12**, 307–330 (1998).
95. Davidson, R. J. Well-being and affective style: Neural substrates and biobehavioural correlates. *Philos. Trans. R. Soc. B Biol. Sci.* **359**, 1395–1411 (2004).
96. Koval, P., Butler, E. A., Hollenstein, T., Lanteigne, D. & Kuppens, P. Emotion regulation and the temporal dynamics of emotions: Effects of cognitive reappraisal and expressive suppression on emotional inertia. *Cogn. Emot.* **29**, 831–851 (2015).
97. Lamm, C. & Singer, T. The role of anterior insular cortex in social emotions. *Brain Struct. Funct.* **214**, 579–591 (2010).

98. Makovac, E., Fagioli, S., Rae, C. L., Critchley, H. D. & Ottaviani, C. Can't get it off my brain: Meta-analysis of neuroimaging studies on perseverative cognition. *Psychiatry Res. - Neuroimaging* **295**, 111020 (2020).
99. Addis, D. R., Wong, A. T. & Schacter, D. L. Remembering the past and imagining the future: Common and distinct neural substrates during event construction and elaboration. *Neuropsychologia* **45**, 1363–1377 (2007).
100. Mason, M. F. *et al.* Wandering minds: The default network and stimulus-independent thought. *Science (80-.).* **315**, 393–395 (2007).
101. Phelps, E. A. & LeDoux, J. E. Contributions of the amygdala to emotion processing: From animal models to human behavior. *Neuron* **48**, 175–187 (2005).
102. Ehring, T. & Watkins, E. R. Repetitive Negative Thinking as a Transdiagnostic Process. *Int. J. Cogn. Ther.* **1**, 192–205 (2008).
103. Jagust, W. Imaging the evolution and pathophysiology of Alzheimer disease. *Nat. Rev. Neurosci.* (2018). doi:10.1038/s41583-018-0067-3
104. Leech, R. & Sharp, D. J. The role of the posterior cingulate cortex in cognition and disease. *Brain* **137**, 12–32 (2014).
105. Critchley, H. D., Wiens, S., Rotshtein, P., Öhman, A. & Dolan, R. J. Neural systems supporting interoceptive awareness. *Nat. Neurosci.* **7**, 189–195 (2004).
106. Zaki, J., Davis, J. I. & Ochsner, K. N. Overlapping activity in anterior insula during interoception and emotional experience. *Neuroimage* **62**, 493–499 (2012).
107. Amodio, D. M. & Frith, C. D. Meeting of minds: The medial frontal cortex and social cognition. *Nature Reviews Neuroscience* **7**, 268–277 (2006).
108. Juchem, C., Nixon, T. W., McIntyre, S., Rothman, D. L. & De Graaf, R. A. Magnetic field homogenization of the human prefrontal cortex with a set of localized electrical coils. *Magn. Reson. Med.* **63**, 171–180 (2010).

ACKNOWLEDGMENTS

The Age-Well randomized clinical trial is part of the Medit-Ageing project and is funded through the European Union's Horizon 2020 Research and Innovation Program (grant agreement n°667696), Institut National de la Santé et de la Recherche Médicale, Région Normandie, and Fondation d'Entreprise MMA des Entrepreneurs du Futur. Institut National de la Santé et de la Recherche Médicale (Inserm) is the sponsor. The funders and sponsor had no role in the design and conduct of the study, collection, management, analysis, and interpretation of the data, preparation, review, or approval of the manuscript, and decision to submit the manuscript for publication. The authors are grateful to the Cyceron staff members for their help with neuroimaging data acquisition; as well as to the EUCLID team, the sponsor (Hélène Espérou – Pôle de recherche Clinique Inserm) and to all the participants in this study for their contribution. We acknowledge and thank the Medit-Ageing Research Group members for their contribution. We thank Clara Bordas, Silvia de Cataldo, and Julia Sachs for their help on the mental thoughts analyses and their dedication during data acquisition. We also thank Bruno Bonnet and Frédéric Grouiller as the principal staff members of the Brain and Behavior Laboratory in Geneva.

AUTHOR CONTRIBUTIONS

Conceptualization: S.B.L., O.K., and P.V.; Data curation: S.B.L., Y.I.D.A., C.M., O.K., and P.V.; Formal analysis: S.B.L., and Y.I.D.A.; Funding acquisition: O.K., N.L.M, G.C., and P.V.; Investigation: S.B.L., C.M., and members of the Medit-Ageing Research Group; Methodology: S.B.L., Y.I.D.A., O.K., G.C., and P.V.; Supervision: O.K., and P.V.; Visualization: S.B.L.; Writing – Original Draft: S.B.L.; Writing – Review and Editing: S.B.L., F.C., G.C., N.L.M., O.K., P.V., C.M., and Y.I.D.A.

COMPETING INTERESTS

Dr. Chételat reported personal fees from Fondation Entrepreneurs MMA and from Fondation Alzheimer. No other disclosures were reported.

MEDIT-AGEING RESEARCH GROUP MEMBERS

SURNAME	FORENAME	EMAIL ADRESS
Arenaza Urquijo	Eider	eiderarenaza@gmail.com
André	Claire	andré@cyceron.fr
Baez Lugo	Sebastian	sebastian.baezlugo@unige.ch
Botton	Maelle	botton@cyceron.fr
Cantou	Pauline	Cantou@cyceron.fr
Chételat	Gaëlle	chetelat@cyceron.fr
Chocat	Anne	annechocat@orange.fr
Collette	Fabienne	f.collette@uliege.be
De la Sayette	Vincent	delasayette-v@chu-caen.fr
Delarue	Marion	delarue@cyceron.fr
Egret	Stéphanie	egret@cyceron.fr
Ferrand Devouge	Eglantine	eglantine.ferranddevouge@gmail.com
Frison	Eric	Eric.Frison@isped.u-bordeaux2.fr
Gonneaud	Julie	gonneaud@cyceron.fr
Heidmann	Marc	marc.heidmann@ens-lyon.fr
Klimecki	Olga	Olga.Klimecki@unige.ch
Kuhn	Elizabeth	kuhn@cyceron.fr
Landeau	Brigitte	landeau@cyceron.fr
Le Du	Gwendoline	ledu@cyceron.fr
Lefranc	Valérie	lefranc@cyceron.fr
Lutz	Antoine	antoine.lutz@inserm.fr
Marchant	Natalie	n.marchant@ucl.ac.uk
Mezenge	Florence	mezenge@cyceron.fr
Moulinet	Inès	moulinet@cyceron.fr
Ourry	Valentin	ourry@cyceron.fr
Poisnel	Géraldine	poisnel@cyceron.fr
Quillard	Anne	anne.quillard@ch-flers.fr
Rauchs	Géraldine	rauchs@cyceron.fr
Rehel	Stéphane	rehel@cyceron.fr
Tomadesso	Clémence	tomadesso@cyceron.fr
Touron	Edelweiss	touron@cyceron.fr
Vuilleumier	Patrik	patrik.vuilleumier@unige.ch
Ware	Caitlin	caitlin.ware@gmail.com
Wirth	Miranka	miranka.wirth@charite.de